

Supporting Information for

Silylene-Assisted Hydride Transfer to CO₂ and CS₂ at a [P₂Si]Ru Pincer-Type Complex

Matthew T. Whited,^{*†} Jia Zhang,[†] Senjie Ma,[†] Binh D. Nguyen,[†] and Daron E. Janzen[‡]

[†] Department of Chemistry, Carleton College, Northfield, MN 55057, United States

[‡] Department of Chemistry and Biochemistry, St. Catherine University, St. Paul, MN 55105, United States

Experimental Section	2
General Considerations	2
(^{Ph} P ₂ Si ^H)Ru(H)(CO)(PPh ₃) (2)	3
(^{Ph} P ₂ Si ^{OTf})Ru(H)(CO)(PPh ₃) (3)	3
[^{(Ph} P ₂ Si ^{OEt2})Ru(H)(CO)(PPh ₃)] [B(C ₆ F ₅) ₄] (4-BArF)	4
[^{(Ph} P ₂ Si=)Ru(H)(CO)(PPh ₃)] [B(C ₆ F ₅) ₄] (5-BArF)	5
[^{(Ph} P ₂ Si ^{O2CH})Ru(CO)(PPh ₃)] [B(C ₆ F ₅) ₄] (6-BArF)	6
[^{(Ph} P ₂ Si ^{S2CH})Ru(CO)(PPh ₃)] [B(C ₆ F ₅) ₄] (7-BArF)	7
Crystallization of [^{(Ph} P ₂ Si ^{S2CH})Ru(CO)(PPh ₃)] [B ₁₂ Cl ₁₂] _{0.5} (7-B₁₂Cl₁₂)	8
Observation of phosphine exchange at (^{Ph} P ₂ Si ^H)Ru(H)(CO)(PPh ₃) (2)	8
Computational Details	8
Figure S1. DFT minimized structure of 5(comp) cation	9
XYZ Coordinates for 5(comp) cation	10
X-ray Crystallography	13
Table S1. X-ray crystallographic data	14
Figure S2. ¹ H NMR spectrum of (^{Ph} P ₂ Si ^H)Ru(H)(CO)(PPh ₃) (2) in C ₆ D ₆	15
Figure S3. ¹³ C{ ¹ H} NMR spectrum of (^{Ph} P ₂ Si ^H)Ru(H)(CO)(PPh ₃) (2) in CD ₂ Cl ₂	16
Figure S4. ²⁹ Si{ ¹ H} NMR spectrum of (^{Ph} P ₂ Si ^H)Ru(H)(CO)(PPh ₃) (2) in CH ₂ Cl ₂	17
Figure S5. ³¹ P{ ¹ H} NMR spectrum of (^{Ph} P ₂ Si ^H)Ru(H)(CO)(PPh ₃) (2) in CH ₂ Cl ₂	18
Figure S6. ¹ H NMR spectrum of (^{Ph} P ₂ Si ^{OTf})Ru(H)(CO)(PPh ₃) (3) in C ₆ D ₆	19
Figure S7. ¹³ C{ ¹ H} NMR spectrum of (^{Ph} P ₂ Si ^{OTf})Ru(H)(CO)(PPh ₃) (3) in CD ₂ Cl ₂	20
Figure S8. ¹⁹ F{ ¹ H} NMR spectrum of (^{Ph} P ₂ Si ^{OTf})Ru(H)(CO)(PPh ₃) (3) in CH ₂ Cl ₂	21
Figure S9. ²⁹ Si{ ¹ H} NMR spectrum of (^{Ph} P ₂ Si ^{OTf})Ru(H)(CO)(PPh ₃) (3) in CH ₂ Cl ₂	22
Figure S10. ³¹ P{ ¹ H} NMR spectrum of (^{Ph} P ₂ Si ^{OTf})Ru(H)(CO)(PPh ₃) (3) in CH ₂ Cl ₂	23
Figure S11. ¹ H NMR spectrum of [^{(Ph} P ₂ Si ^{OEt2})Ru(H)(CO)(PPh ₃)] [BArF] (4-BArF) in C ₆ D ₆ :C ₆ D ₅ Br [1:1]	24
Figure S12. ²⁹ Si{ ¹ H} NMR spectrum of [^{(Ph} P ₂ Si ^{OEt2})Ru(H)(CO)(PPh ₃)] [BArF] (4-BArF) in C ₆ H ₅ F	25
Figure S13. ³¹ P{ ¹ H} NMR spectrum of [^{(Ph} P ₂ Si ^{OEt2})Ru(H)(CO)(PPh ₃)] [BArF] (4-BArF) in C ₆ H ₅ F	26
Figure S14. ¹ H NMR spectrum of [^{(Ph} P ₂ Si=)Ru(H)(CO)(PPh ₃)] [BArF] (5-BArF) in C ₆ D ₆	27
Figure S15. ²⁹ Si{ ¹ H} NMR spectrum of [^{(Ph} P ₂ Si=)Ru(H)(CO)(PPh ₃)] [BArF] (5-BArF) in C ₆ H ₅ F	28
Figure S16. ³¹ P{ ¹ H} NMR spectrum of [^{(Ph} P ₂ Si=)Ru(H)(CO)(PPh ₃)] [BArF] (5-BArF) in C ₆ H ₅ F	29
Figure S17. ¹ H NMR spectrum of [^{(Ph} P ₂ Si ^{O2CH})Ru(CO)(PPh ₃)] [BArF] (6-BArF) in C ₆ D ₅ Br	30
Figure S18. ²⁹ Si{ ¹ H} NMR spectrum of [^{(Ph} P ₂ Si ^{O2CH})Ru(CO)(PPh ₃)] [BArF] (6-BArF) in C ₆ D ₆ :C ₆ H ₅ F [1:1]	31
Figure S19. ³¹ P{ ¹ H} NMR spectrum of [^{(Ph} P ₂ Si ^{O2CH})Ru(CO)(PPh ₃)] [BArF] (6-BArF) in C ₆ H ₅ F	32
Figure S20. ¹ H NMR spectrum of crude ¹³ C-[^{(Ph} P ₂ Si ^{O2CH})Ru(CO)(PPh ₃)] [BArF] (6(¹³C)-BArF) in C ₆ D ₅ Br	33
Figure S21. ¹³ C NMR spectrum of crude ¹³ C-[^{(Ph} P ₂ Si ^{O2CH})Ru(CO)(PPh ₃)] [BArF] (6(¹³C)-BArF) in C ₆ D ₅ Br	34
Figure S22. ³¹ P NMR spectrum of crude ¹³ C-[^{(Ph} P ₂ Si ^{O2CH})Ru(CO)(PPh ₃)] [BArF] (6(¹³C)-BArF) in C ₆ H ₅ F	35
Figure S23. ¹ H NMR spectrum of [^{(Ph} P ₂ Si ^{S2CH})Ru(CO)(PPh ₃)] [BArF] (7-BArF) in C ₆ D ₅ Br	36
Figure S24. ²⁹ Si NMR spectrum of [^{(Ph} P ₂ Si ^{S2CH})Ru(CO)(PPh ₃)] [BArF] (7-BArF) in C ₆ D ₆ :C ₆ H ₅ F [1:1]	37

Figure S25. ^{31}P NMR spectrum of $[({}^{\text{Ph}}\text{P}_2\text{Si}^{\text{S}2\text{CH}})\text{Ru}(\text{CO})(\text{PPh}_3)][\text{BArF}]$ (7-BArF) in $\text{C}_6\text{H}_5\text{F}$	38
Figure S26. Infrared spectrum of $({}^{\text{Ph}}\text{P}_2\text{Si}^{\text{H}})\text{Ru}(\text{H})(\text{CO})(\text{PPh}_3)$ in CH_2Cl_2	39
Figure S27. Infrared spectrum of $({}^{\text{Ph}}\text{P}_2\text{Si}^{\text{OTf}})\text{Ru}(\text{H})(\text{CO})(\text{PPh}_3)$ in CH_2Cl_2	40
Figure S28. Infrared spectrum of $[({}^{\text{Ph}}\text{P}_2\text{Si}^{\text{OEt}2})\text{Ru}(\text{H})(\text{CO})(\text{PPh}_3)][\text{BArF}]$ in CH_2Cl_2	41
Figure S29. Infrared spectrum of $[({}^{\text{Ph}}\text{P}_2\text{Si}=\text{)}\text{Ru}(\text{H})(\text{CO})(\text{PPh}_3)][\text{BArF}]$ in CH_2Cl_2	42
Figure S30. Infrared spectrum of $[({}^{\text{Ph}}\text{P}_2\text{Si}^{\text{O}2\text{CH}})\text{Ru}(\text{H})(\text{CO})(\text{PPh}_3)][\text{BArF}]$ in CH_2Cl_2	43
Figure S31. Infrared spectrum of $^{13}\text{C}-[({}^{\text{Ph}}\text{P}_2\text{Si}^{\text{O}2\text{CH}})\text{Ru}(\text{H})(\text{CO})(\text{PPh}_3)][\text{BArF}]$ in CH_2Cl_2	44
Figure S32. Infrared spectrum of $[({}^{\text{Ph}}\text{P}_2\text{Si}^{\text{S}2\text{CH}})\text{Ru}(\text{H})(\text{CO})(\text{PPh}_3)][\text{BArF}]$ in CH_2Cl_2	45
Figure S33. ^{31}P NMR spectra of reaction of 2 with tri(<i>p</i> -tolyl)phosphine in $\text{C}_6\text{H}_5\text{F}$	46
References	47

Experimental Section

General Considerations. All manipulations were carried out under a dinitrogen atmosphere in an MBraun Unilab 2000 glove box or under an argon atmosphere using standard Schlenk techniques. Routine solvents were purchased from Aldrich and were deoxygenated and dried using a Glass Contour Solvent Purification System, except for anhydrous benzene and pentane, which were used as received from Aldrich. $\text{Cs}_2\text{B}_{12}\text{Cl}_{12}$ was prepared according to literature procedures,¹ converted to $\text{Ag}_2\text{B}_{12}\text{Cl}_{12}$ by reaction with silver nitrate in water, and further converted to the tetra-*n*-butylammonium salt by reaction with tetra-*n*-butylammonium bromide in dichloromethane in an inert-atmosphere glove box. The $[{}^{\text{Ph}}\text{P}_2\text{Si}]\text{H}_2$ ligand,² trityl triflate,³ and trityl BArF (BArF = $\text{B}(\text{C}_6\text{F}_5)_4^-$)⁴ were prepared according to published methods. NMR solvents (Cambridge Isotope Labs) were degassed and passed through a pad of activated alumina prior to use (benzene-*d*₆) or vacuum transferred from sodium/benzophenone (bromobenzene-*d*₅ and dichloromethane-*d*₂). Alumina was activated by heating at 300 °C for 8–12 h under vacuum prior to use. Other reagents were purchased from commercial vendors and used without further purification. NMR spectra were recorded at ambient temperature on a Bruker Avance III HD 400 High Performance Digital NMR spectrometer. ^1H and ^{13}C NMR chemical shifts were referenced to residual solvent, ^{29}Si and ^{31}P NMR chemical shifts are reported relative to external standards of 85% H_3PO_4 and tetramethylsilane, respectively. IR spectra were recorded on a Mattson 4020 Galaxy Series or

Thermo Scientific Nicolet iS5 FTIR spectrometer in CH_2Cl_2 using a solution IR cell with NaCl windows. Microanalysis was carried out by Midwest Microlab, LLC.

($^{\text{Ph}}\text{P}_2\text{Si}^{\text{H}}$)Ru(H)(CO)(PPh₃) (2). Carbonyl(dihydrido)tris(triphenylphosphine)ruthenium (238 mg, 0.260 mmol) and the ($^{\text{Ph}}\text{P}_2\text{Si}$)H₂ ligand (143 mg, 0.259 mmol) were combined in benzene (15 mL) and heated at 80°C for 16 h with stirring in a sealed vial. The reaction mixture was concentrated *in vacuo* to a white powder, which was washed with pentane (3 × 10 mL) to remove triphenylphosphine. The crude product was redissolved in minimal dichloromethane and crystallized by vapor diffusion with pentane at -38°C, affording pure **1** as a crop of colorless crystals. Yield: 199 mg, 81 %. ¹H NMR (400 MHz, C₆D₆): δ 8.47 (d, *J* = 7.3 Hz, 2H), 7.27–7.16 (m, 11H), 7.13–7.07 (dt, *J*₁ = 7.7 Hz, *J*₂ = 3.8 Hz, 2H), 7.02–6.77 (m, 24H), 6.69–6.60 (m, 5H, Si-H and Ar-H), -7.64 (td, ²*J*_{HP} = 28.9 Hz, ²*J*_{HP} = 12.2 Hz, 1H, Ru-H). ¹³C{¹H} (101 MHz, CD₂Cl₂): δ 207.3 (q, ²*J*_{CP} = 7 Hz, Ru-CO), 152.5 (td, *J*₁ = 30 Hz, 8 Hz), 151.5 (td, *J* = 25 Hz, 2 Hz), 139.1 (t, *J* = 17 Hz), 138.4 (td, *J* = 21 Hz, 5 Hz), 134.4–134.3 (m), 134.2 (t, *J* = 6 Hz), 133.4 (td, *J* = 10 Hz, 2 Hz), 132.4 (t, *J* = 6 Hz), 131.7 (t, *J* = 3 Hz), 129.5, 129.2, 128.8, 128.7, 128.5 (t, *J* = 5 Hz), 128.0 (t, *J* = 4 Hz), 128.0, 127.9, 127.7 (t, *J* = 5 Hz). ²⁹Si{¹H} NMR (79 MHz, C₆D₆): δ 47.3 (dt, ²*J*_{SiP} = 83 Hz, ²*J*_{SiP} = 15 Hz). ³¹P{¹H} NMR (162 MHz, C₆D₆): δ 65.7 (d, ²*J*_{PP} = 21 Hz), 41.0 (t, ²*J*_{PP} = 21 Hz, Ru-PPh₃). IR (CH₂Cl₂, cm⁻¹): ν 2024 (SiH), 1942 (CO). Anal. calcd. for C₅₅H₄₅OP₃RuSi: C, 69.98; H, 4.80. Found: C, 70.12; H, 5.02.

($^{\text{Ph}}\text{P}_2\text{Si}^{\text{OTf}}$)Ru(H)(CO)(PPh₃) (3). Complex **2** (14.4 mg, 0.015 mmol) and trityl triflate (6.00 mg, 0.015 mmol) were separately dissolved in dichloromethane (5 mL each) and chilled to -38 °C. The trityl triflate solution was added dropwise to the solution of **2**, causing the solution to

adopt a slightly yellow hue. Volatiles were removed *in vacuo* and the resulting yellow solid was washed with pentane (3×5 mL) to remove triphenylmethane. The resulting product was redissolved in minimal dichloromethane and crystallized by vapor diffusion with pentane at -38°C . Yield: 19.0 mg, 95 %. The crystals of **3** obtained from dichloromethane as the CH_2Cl_2 solvate suffered from severe disorder of the triflate unit, but a small crop of colorless crystals of **3** suitable for X-ray analysis was obtained from a concentrated toluene solution by vapor diffusion with pentane at -38°C . ^1H NMR (400 MHz, C_6D_6): δ 8.92 (d, $J = 7.5$ Hz, 2H), 7.22 (td, $J = 7.4$ Hz, 1.3 Hz, 2H), 7.16–7.03 (m, 14H), 7.02–6.91 (m, 6H), 6.90–6.81 (m, 3H), 6.82–6.72 (m, 13H), 6.58 (t, $J = 7.7$ Hz, 4H), –8.22 (td, $^2J_{\text{HP}} = 26.9$ Hz, $^2J_{\text{HP}} = 11.5$ Hz, 1H, Ru–H). $^{13}\text{C}\{^1\text{H}\}$ (101 MHz, CD_2Cl_2): δ 204 (Ru–CO), 152.8 (td, $J_1 = 29$ Hz, 6 Hz), 148.5 (td, $J = 23$ Hz, 5 Hz), 136.7 (t, $J = 19$ Hz), 136.6 (td, $J = 22$ Hz, 3 Hz), 133.6 (t, $J = 6$ Hz), 132.5 (t, $J = 9$ Hz), 131.9 (t, $J = 2$ Hz), 129.3 (t, $J = 4$ Hz), 129.5, 129.1, 129.0, 128.9, 128.3, 128.0 (t, $J = 5$ Hz), 127.6, 127.5, 127.3 (t, $J = 5$ Hz). $^{19}\text{F}\{^1\text{H}\}$ NMR (376 MHz, C_6D_6): δ 78.1. $^{29}\text{Si}\{^1\text{H}\}$ NMR (79 MHz, C_6D_6): δ 114.7 (dt, $^2J_{\text{SiP}} = 110$ Hz, $^2J_{\text{SiP}} = 19$ Hz). $^{31}\text{P}\{^1\text{H}\}$ NMR (162 MHz, C_6D_6): δ 64.1 (d, $^2J_{\text{PP}} = 23$ Hz), 39.2 (t, $^2J_{\text{PP}} = 23$ Hz, Ru– $P\text{Ph}_3$). IR (CH_2Cl_2 , cm^{-1}): ν 1965 (CO). Anal. calcd. for $\text{C}_{56}\text{H}_{44}\text{F}_3\text{O}_4\text{P}_3\text{RuSSi}\cdot\text{CH}_2\text{Cl}_2$: C, 58.16; H, 3.94. Found: C, 57.20; H, 4.20. NOTE: Complex **3** crystallized with two molecules of dichloromethane solvent per asymmetric unit, but elemental analysis indicates that some of this solvent (0.7 equiv) was removed during drying.

[$(^{\text{Ph}}\text{P}_2\text{Si}^{\text{OE}t_2})\text{Ru}(\text{H})(\text{CO})(\text{PPh}_3)\text{][B(C}_6\text{F}_5)_4\text{]}$ (4-BArF). Complex **2** (14.4 mg, 0.015 mmol) and trityl BArF (14.2 mg, 0.015 mmol) were separately dissolved in fluorobenzene (5 mL) and chilled to -38°C . The trityl BArF solution was added dropwise to the solution of **1** with stirring, causing it to adopt a slight yellow hue. After several minutes, a solution of diethyl ether (60 μL , 0.30 mM

in fluorobenzene, 0.018 mmol) was added. The mixture was allowed to stir for 5 min, then volatiles were removed *in vacuo*. The resulting yellow solid was dissolved in benzene and lyophilized, then washed with pentane (3×5 mL) to remove triphenylmethane and dried *in vacuo* over 48 h. Yield: 22.6 mg, 89%. ^1H NMR (400 MHz, $\text{C}_6\text{D}_6/\text{C}_6\text{D}_5\text{Br}$ [1:1]): δ 8.14 (d, $J = 7.4$ Hz, 2H), 7.33 (m, 4H), 7.22–6.78 (m, 27H), 7.02–6.91 (m, 6H), 6.70–6.58 (m, 6H), 6.36 (br s, 4H), 3.50 (q, $^3J_{\text{HH}} = 7.0$ Hz, 4H, Si–O(CH_2CH_3)₂), 0.53 (t, $^3J_{\text{HH}} = 7.0$ Hz, 6H, Si–O(CH_2CH_3)₂), –8.38 (td, $^2J_{\text{HP}} = 27.6$ Hz, $^2J_{\text{HP}} = 10.9$ Hz, 1H, Ru–H). $^{29}\text{Si}\{\text{H}\}$ NMR (79 MHz, C_6D_6): δ 150.7 (dt, $^2J_{\text{SiP}} = 112$ Hz, $^2J_{\text{SiP}} = 18$ Hz). $^{31}\text{P}\{\text{H}\}$ NMR (162 MHz, C_6D_6): δ 64.2 (d, $^2J_{\text{PP}} = 24$ Hz), 37.0 (t, $^2J_{\text{PP}} = 24$ Hz, Ru– PPh_3). IR (CH_2Cl_2 , cm^{-1}): ν 1955 (CO). Attempted microanalysis of **4-BArF** suggested that the pure compound precipitated with some amount of solvent that could not easily be removed or definitively quantified. For instance, after precipitation of **4-BArF** with pentane from a concentrated dichloromethane solution, microanalysis was consistent with the inclusion of one-half equivalent of CH_2Cl_2 : Anal. calcd. for $\text{C}_{83}\text{H}_{54}\text{BF}_{20}\text{O}_2\text{P}_3\text{RuSi}\cdot 0.5\text{CH}_2\text{Cl}_2$: C, 57.68; H, 3.19. Found: C, 57.72; H, 3.24. Although this microanalysis is not definitive for the proposed formulation, the fact that **4-BArF** can be cleanly generated from **5-BArF**, combined with the weight of the spectral evidence for both species, confirms the formulation.

[$(^{\text{Ph}}\text{P}_2\text{Si=})\text{Ru}(\text{H})(\text{CO})(\text{PPh}_3)]\text{[B(C}_6\text{F}_5)_4]$ (5-BArF**).** Complex **2** (14.4 mg, 0.015 mmol) and trityl BArF (14.2 mg, 0.015 mmol) were separately dissolved in fluorobenzene (5 mL) and chilled to -38 °C. The trityl BArF solution was added dropwise to the solution of **1**, causing the solution to adopt a yellow hue. Pentane (ca. 5 mL) was added, causing **5** to precipitate as a yellow solid, which was isolated by filtration. Yield: 22.4 mg, 88 %. ^1H NMR (400 MHz, C_6D_6): δ 8.13 (d, $J = 7.4$ Hz, 2H), 7.29 (t, $J = 7.3$ Hz, 2H), 7.16–7.03 (m, 14H), 6.57 (t, $J = 7.5$ Hz, 4H), 6.46 (q, $J = 5.8$

Hz, 4H), –7.89 (t, $^2J_{\text{HP}} = 15.3$ Hz, 1H, Ru–H). $^{29}\text{Si}\{\text{H}\}$ NMR (79 MHz, C_6D_6): δ 278 (d, $^2J_{\text{SiP}} = 108$ Hz). $^{31}\text{P}\{\text{H}\}$ NMR (162 MHz, C_6D_6): δ 55.8 (d, $^2J_{\text{PP}} = 21$ Hz), 37.7 (t, $^2J_{\text{PP}} = 21$ Hz, Ru– $P\text{Ph}_3$). IR (CH_2Cl_2 , cm^{-1}): ν 1979 (CO). Anal. calcd. for $\text{C}_{79}\text{H}_{44}\text{BF}_{20}\text{OP}_3\text{RuSi}\cdot\text{C}_5\text{H}_{12}$: C, 59.55; H, 3.33. Found: C, 59.95; H, 3.37. NOTE: The BArF salts **5-BArF**, **6-BArF**, and **7-BArF** were precipitated with pentane, and microanalysis revealed a single equivalent of pentane was retained upon isolation.

[($^{\text{Ph}}\text{P}_2\text{SiO}^{2\text{CH}}$)Ru(CO)(PPh₃)] [B(C₆F₅)₄] (6-BArF). Complex **2** (14.4 mg, 0.015 mmol) and trityl BArF (14.2 mg, 0.015 mmol) were separately dissolved in fluorobenzene (5 mL) and chilled to –38 °C. The trityl BArF solution was added dropwise to the solution of **2**, causing the solution to adopt a yellow hue. The volume of the resulting solution was reduced to ca. 0.75 mL *in vacuo* and it was transferred to a J Young NMR tube. The solution was subjected to one freeze–pump–thaw cycle and the headspace was backfilled with CO₂. The reaction was allowed to proceed 16 h, then the mixture was brought back into the glove box, dried *in vacuo*, and triturated with pentane (3 × 5 mL) to remove triphenylmethane, affording **6-BArF** as a pale yellow solid. Yield: 21.5 mg, 86 %. In order to isolate **5** as a powder suitable for elemental analysis, the product was redissolved in minimal fluorobenzene and precipitated with pentane. ^1H NMR (400 MHz, $\text{C}_6\text{D}_5\text{Br}$): δ 8.34 (d, $J = 7.4$ Hz, 2H), 7.37 (t, $J = 7.5$ Hz, 2H), 7.18–6.97 (m, 22H), 6.94–6.90 (m, 4H), 6.87–6.80 (m, 9H), 6.32 (s, 1H, O₂CH), 6.17 (q, $J = 5.6$ Hz, 4H). $^{29}\text{Si}\{\text{H}\}$ NMR (79 MHz, $\text{C}_6\text{D}_5\text{Br}$): δ 118 (dt, $^2J_{\text{SiP}} = 96$ Hz, $^2J_{\text{SiP}} = 12$ Hz). $^{31}\text{P}\{\text{H}\}$ NMR (162 MHz, $\text{C}_6\text{D}_6\cdot\text{C}_6\text{H}_5\text{F}$ [1:1]): δ 51.3 (d, $^2J_{\text{PP}} = 20$ Hz), 14.5 (t, $^2J_{\text{PP}} = 20$ Hz, Ru–PPh₃). IR (CH_2Cl_2 , cm^{-1}): ν 1955 (CO), 1577 (OCO). Selected NMR spectral data for ¹³C-labelled product: ^1H NMR (400 MHz, $\text{C}_6\text{D}_5\text{Br}$): δ 6.32 (d, $^1J_{\text{HC}} = 232$ Hz, 1H, O₂¹³CH). ^{13}C NMR (101 MHz, $\text{C}_6\text{D}_5\text{Br}$): δ 171.6 (dd, $^1J_{\text{CH}} = 232$ Hz, $^3J_{\text{CP}} = 8$ Hz, O₂CH). $^{31}\text{P}\{\text{H}\}$

NMR (162 MHz, C₆H₅F): δ 51.3 (d, ²J_{PP} = 20 Hz), 14.5 (td, ²J_{PP} = 20 Hz, ³J_{PC} = 8 Hz). IR (CH₂Cl₂, cm⁻¹): ν 1955 (CO), 1538 (OCO). Anal. calcd. for C₈₀H₄₄BF₂₀O₃P₃RuSi·C₅H₁₂: C, 58.73; H, 3.25. Found: C, 58.77; H, 3.02. NOTE: The BArF salts **5-BArF**, **6-BArF**, and **7-BArF** were precipitated with pentane, and microanalysis revealed a single equivalent of pentane was retained upon isolation.

[(^{Ph}P₂Si^{S2CH})Ru(CO)(PPh₃)][B(C₆F₅)₄] (7-BArF). Complex **2** (14.4 mg, 0.015 mmol) and trityl BArF (14.2 mg, 0.015 mmol) were separately dissolved in fluorobenzene (5 mL) and chilled to -38 °C. The trityl BArF solution was added dropwise to the solution of **2**, causing the solution to adopt a yellow hue. After several minutes, a solution of carbon disulfide (50 μL, 0.44 mM in fluorobenzene, 0.022 mmol) was added and the reaction allowed to proceed 5 min. Volatiles were removed *in vacuo* and the resulting yellow solid was triturated with pentane (3 × 5 mL) to remove triphenylmethane. Yield: 23.2 mg, 92 %. In order to isolate **6** as a powder suitable for elemental analysis, the product was redissolved in minimal fluorobenzene and precipitated with pentane. ¹H NMR (400 MHz, C₆D₅Br): δ 9.61 (s, 1H, S₂CH), 8.26 (d, J = 7.5 Hz, 2H), 7.29 (t, J = 7.3 Hz, 2H), 7.20–6.97 (m, 14H), 6.88–6.74 (m, 17H), 6.69 (q, J = 6.2 Hz, 4H), 6.08 (q, J = 6.2 Hz, 4H). ²⁹Si{¹H} NMR (79 MHz, C₆D₆:C₆H₅F [1:1]): δ 117 (dt, ²J_{SiP} = 98 Hz, ²J_{SiP} = 12 Hz). ³¹P{¹H} NMR (162 MHz, C₆H₅F): δ 50.6 (d, ²J_{PP} = 19 Hz), 18.9 (t, ²J_{PP} = 19 Hz, Ru-PPh₃). IR (CH₂Cl₂, cm⁻¹): ν 1973 (CO). Anal. calcd. for C₈₀H₄₄BF₂₀OP₃RuS₂Si·C₅H₁₂: C, 57.67; H, 3.19. Found: C, 57.52; H, 3.11. NOTE: The BArF salts **5-BArF**, **6-BArF**, and **7-BArF** were precipitated with pentane, and microanalysis revealed a single equivalent of pentane was retained upon isolation.

Crystallization of $[({}^{\text{Ph}}\text{P}_2\text{Si}^{\text{S}2\text{CH}})\text{Ru}(\text{CO})(\text{PPh}_3)][\text{B}_{12}\text{Cl}_{12}]_{0.5}$ (7-B₁₂Cl₁₂).

Crystals of **7** were obtained as the dodecachlorododecaborate ($\text{B}_{12}\text{Cl}_{12}^{2-}$) salt by dissolving **7-BArF** in ca. 3 mL of a concentrated solution of tetra-*n*-butylammonium dodecachlorododecaborate ($\text{TBA}_2\text{B}_{12}\text{Cl}_{12}$) in THF and storing at –35 °C for two weeks.

Observation of phosphine exchange at $({}^{\text{Ph}}\text{P}_2\text{Si}^{\text{H}})\text{Ru}(\text{H})(\text{CO})(\text{PPh}_3)$ (2). Two a solution of complex **2** (20.9 mg, 0.022 mmol) in fluorobenzene (0.8 mL) was added a solution of tri(*p*-tolyl)phosphine (20.1 mg, 0.066 mmol). The mixture was transferred to an NMR tube and no reaction occurred over a period of 12 h, as judged by ${}^{31}\text{P}$ NMR spectroscopy. The mixture was heated at 80 °C and periodically examined by ${}^{31}\text{P}$ NMR spectroscopy, showing slow conversion to a 40:60 mixture of **2** and $({}^{\text{Ph}}\text{P}_2\text{Si}^{\text{H}})\text{Ru}(\text{H})(\text{CO})(\text{P}(p\text{-tol})_3)$ over a period of 60 h. ${}^{31}\text{P}$ NMR spectra for this reaction are presented in Figure S33.

Computational Details. All DFT calculations were performed using Gaussian09⁵ using the M06 functional⁶ and the def2SVP basis set⁷ with effective core potentials for Ru.⁸ Geometries were optimized in the gas phase. A rendering of the **5(comp)** cation is presented below (Figure S1) along with XYZ coordinates.

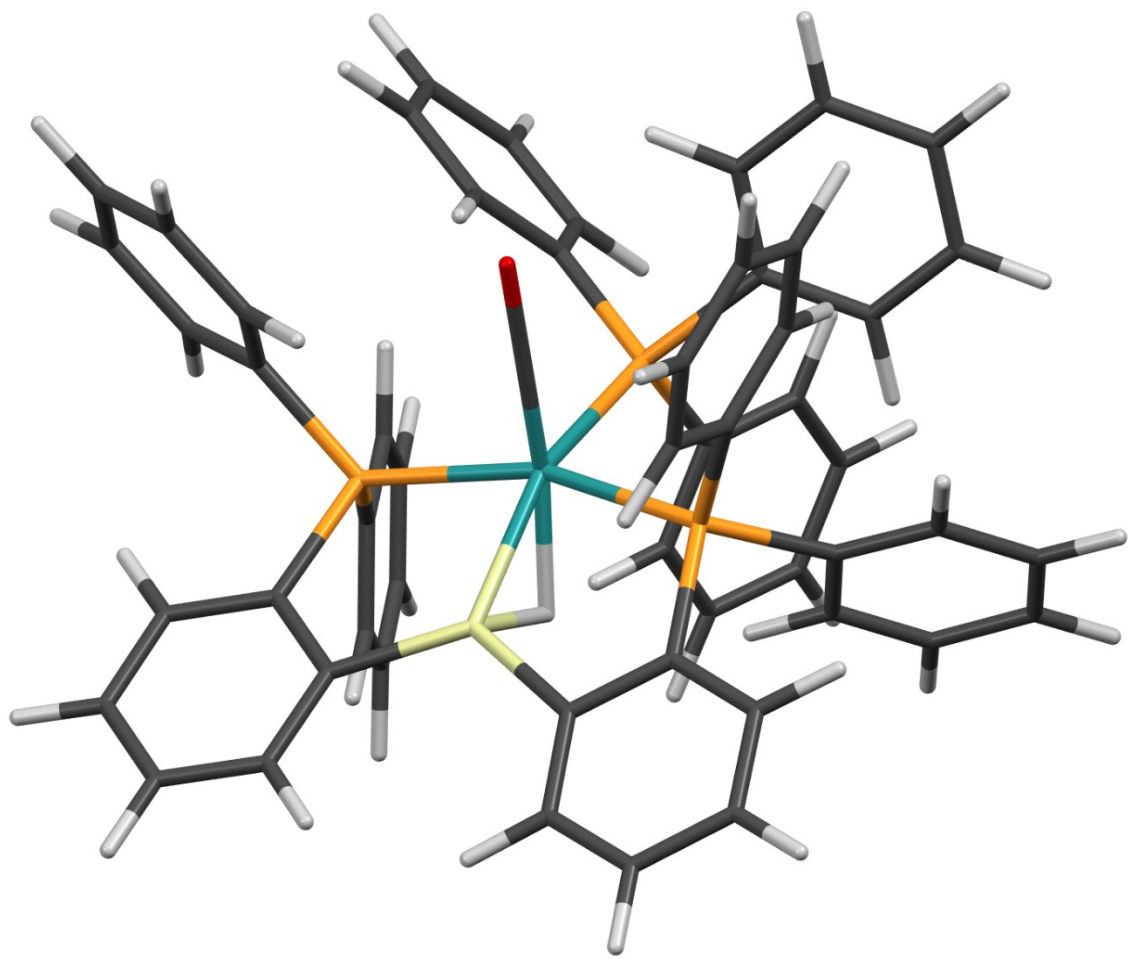


Figure S1. DFT minimized structure of **5(comp)** cation

XYZ Coordinates for 5(comp) cation

Ru	0.000000	0.000000	0.000000
H	0.079440	0.628628	-1.705254
P	2.403687	0.297087	-0.194119
C	3.521692	0.074054	1.242137
C	4.788691	-0.512191	1.152707
H	5.157497	-0.899296	0.198425
C	5.598359	-0.601772	2.283951
C	5.155340	-0.104776	3.506795
H	5.793022	-0.178376	4.391980
C	3.901959	0.499695	3.597404
C	3.090713	0.591113	2.470626
H	2.114712	1.082663	2.547160
H	3.553102	0.905636	4.550763
H	6.586822	-1.062798	2.204242
C	2.780817	2.056190	-0.668000
C	1.719586	2.920687	-0.996963
Si	0.063650	2.118037	-0.735903
C	-1.537823	2.947381	-1.187517
C	-2.640879	2.125568	-0.890394
P	-2.348889	0.438559	-0.167464
C	-3.393224	-0.565432	-1.292086
C	-2.832952	-0.924573	-2.523747
H	-1.800807	-0.640449	-2.757558
C	-3.572775	-1.653082	-3.449939
H	-3.116741	-1.939821	-4.402398
C	-4.887139	-2.016448	-3.156741
H	-5.471374	-2.590632	-3.881121
C	-5.459786	-1.637901	-1.943850
C	-4.718117	-0.914816	-1.011069
H	-5.176650	-0.628799	-0.058879
H	-6.495371	-1.908517	-1.718682
C	-3.190718	0.508397	1.451002
C	-3.276898	1.721128	2.144943
H	-2.955669	2.655066	1.670868
C	-3.763349	1.747934	3.449609
H	-3.826600	2.699781	3.983921
C	-4.167813	0.568813	4.070500
C	-4.079346	-0.641218	3.385269
H	-4.391592	-1.572363	3.867352
C	-3.585905	-0.676444	2.084625
H	-3.504004	-1.638219	1.568652
H	-4.550176	0.592612	5.094494
C	-3.937795	2.567905	-1.158059
H	-4.797549	1.925089	-0.938928
C	-4.139572	3.833993	-1.702107

H	-5.156859	4.181738	-1.901928
C	-3.052248	4.656629	-1.997432
H	-3.217136	5.646363	-2.431804
C	-1.757476	4.214656	-1.745183
H	-0.912831	4.865389	-1.992651
C	2.003372	4.237723	-1.382763
C	3.319110	4.686671	-1.440503
H	3.533053	5.717521	-1.735231
C	4.364394	3.822539	-1.114920
H	5.398119	4.176783	-1.154406
C	4.099399	2.509428	-0.732233
H	4.926965	1.838827	-0.475563
H	1.191856	4.928090	-1.633457
C	3.153825	-0.613649	-1.603006
C	3.213552	-0.015380	-2.869569
H	2.903438	1.026260	-3.005987
C	3.673196	-0.735204	-3.969817
C	4.077925	-2.060710	-3.823753
H	4.441247	-2.623237	-4.688099
C	4.019420	-2.663545	-2.569414
C	3.560065	-1.947342	-1.467059
H	3.523448	-2.440019	-0.492335
H	4.333162	-3.703484	-2.438592
H	3.722415	-0.250627	-4.949128
P	-0.078233	-2.472453	-0.266051
C	-0.152592	-3.121234	-1.985280
C	-0.625245	-4.407617	-2.284970
H	-0.981579	-5.065668	-1.485614
C	-0.649953	-4.862284	-3.600550
C	-0.192773	-4.045261	-4.633960
C	0.294041	-2.773120	-4.345056
C	0.310293	-2.314717	-3.029377
H	0.684432	-1.307942	-2.810338
H	0.668293	-2.128155	-5.145543
H	-0.212720	-4.405113	-5.666508
H	-1.026847	-5.865345	-3.819086
C	1.338608	-3.392556	0.489327
C	1.919184	-2.900730	1.665311
H	1.547470	-1.978226	2.120655
C	2.985504	-3.564913	2.268151
C	3.494030	-4.728555	1.696299
H	4.334823	-5.248888	2.163263
C	2.922597	-5.228108	0.526927
C	1.850857	-4.569303	-0.070895
H	1.432428	-4.970037	-0.998660
H	3.314762	-6.142808	0.072985

H	3.422255	-3.160989	3.186511
C	-1.506514	-3.285036	0.580257
C	-2.709485	-3.550527	-0.087834
H	-2.816915	-3.319961	-1.151954
C	-3.782025	-4.129489	0.588494
C	-3.676835	-4.440019	1.942230
C	-2.490640	-4.162705	2.619373
C	-1.415333	-3.589649	1.945454
H	-0.490632	-3.391129	2.496345
H	-2.394373	-4.401645	3.682182
H	-4.516234	-4.903808	2.467920
H	-4.706767	-4.341695	0.043555
C	-0.138832	-0.147368	1.864213
O	-0.264691	-0.169912	3.010684

X-ray Crystallography. Single-crystal X-ray diffraction data for compounds **2** and **3** were collected on a Rigaku XtaLAB mini diffractometer using Mo K α radiation ($\lambda = 0.71073 \text{ \AA}$). The diffractometer was equipped with an Oxford Cryosystems desktop cooler (Oxford Cryosystems Ltd, Oxford) for low-temperature data collection. The crystals were mounted on a MiTeGen micromount (MiTeGen, LLC, Ithaca, NY) using STP oil. The frames were integrated using CrystalClear-SM Expert 3.1 b27⁹ to give the *hkl* files corrected for *Lp* and decay. Data were corrected for absorption effects using a multiscan method (REQAB).⁹

Single-crystal X-ray diffraction data for compound **7-B₁₂Cl₁₂** were collected at the University of Minnesota X-ray crystallographic laboratory on a Bruker APEX II Platform CCD diffractometer using Mo K α radiation ($\lambda = 0.71073 \text{ \AA}$). The data intensities were corrected for absorption and decay (SADABS). Final cell constants were obtained from least-squares fits of all measured reflection.

All structures were solved using SHELXS-2013 and refined using SHELXL-2013 with the Olex2 software package.¹⁰ All non-hydrogen atoms were refined with anisotropic thermal parameters. Ruthenium and silicon hydrides were located in the Fourier difference maps and refined isotropically; all other hydrogen atoms were inferred geometrically from neighboring sites and refined with riding thermal parameters. Crystallographic parameters of all complexes are summarized in Table S1. ORTEP drawings were prepared using ORTEP-3 for Windows V2013.1¹¹ and POV-Ray for Windows v3.6.¹² Crystallographic data for the complexes have been deposited at the Cambridge Crystallographic Data Centre (Nos. 1566072–1566074) and can be obtained free of charge via www.ccdc.cam.ac.uk.

Table S1. X-ray crystallographic data

complex	2	3	7-B₁₂Cl₁₂
Empirical Formula	C ₅₅ H ₄₅ OP ₃ RuSi·2CH ₂ Cl ₂	C ₅₆ H ₄₄ F ₃ O ₄ P ₃ RuSSi·C ₇ H ₈	C ₅₆ H ₄₄ OP ₃ RuS ₂ Si·(B ₁₂ Cl ₂) _{0.5}
Formula Weight	1113.83	1184.17	1296.66
T (K)	173(2)	173(2)	173(2)
Crystal System	Monoclinic	Triclinic	Monoclinic
Space Group	P2 ₁ /c	P ¹	C2/c
<i>a</i> (Å)	12.5608(10)	13.1211(17)	28.1350(19)
<i>b</i> (Å)	17.3752(14)	13.5719(18)	17.6566(12)
<i>c</i> (Å)	23.586(2)	17.210(2)	29.6568(19)
α (deg)	90	108.220(8)	90
β (deg)	92.353(6)	103.018(7)	105.892(2)
γ (deg)	90	94.303(7)	90
<i>V</i> (Å ³)	5143.3(7)	2800.9(7)	14169.5(16)
<i>Z</i>	4	2	8
<i>d</i> _{calc} (g/cm ³)	1.438	1.404	1.216
μ (mm ⁻¹)	0.670	0.482	0.624
Reflections Collected	38363	23813	102808
Independent Reflections	10502 [R(int) = 0.0712]	9875 [R(int) = 0.0888]	21672 [R(int) = 0.0648]
Data / Restraints / Parameters	10502 / 0 / 612	9875 / 45 / 690	21672 / 0 / 685
GOF on F ²	1.026	1.022	1.026
R1 (wR2)	0.0489 (0.1008)	0.0607 (0.1446)	0.0642 (0.1699)

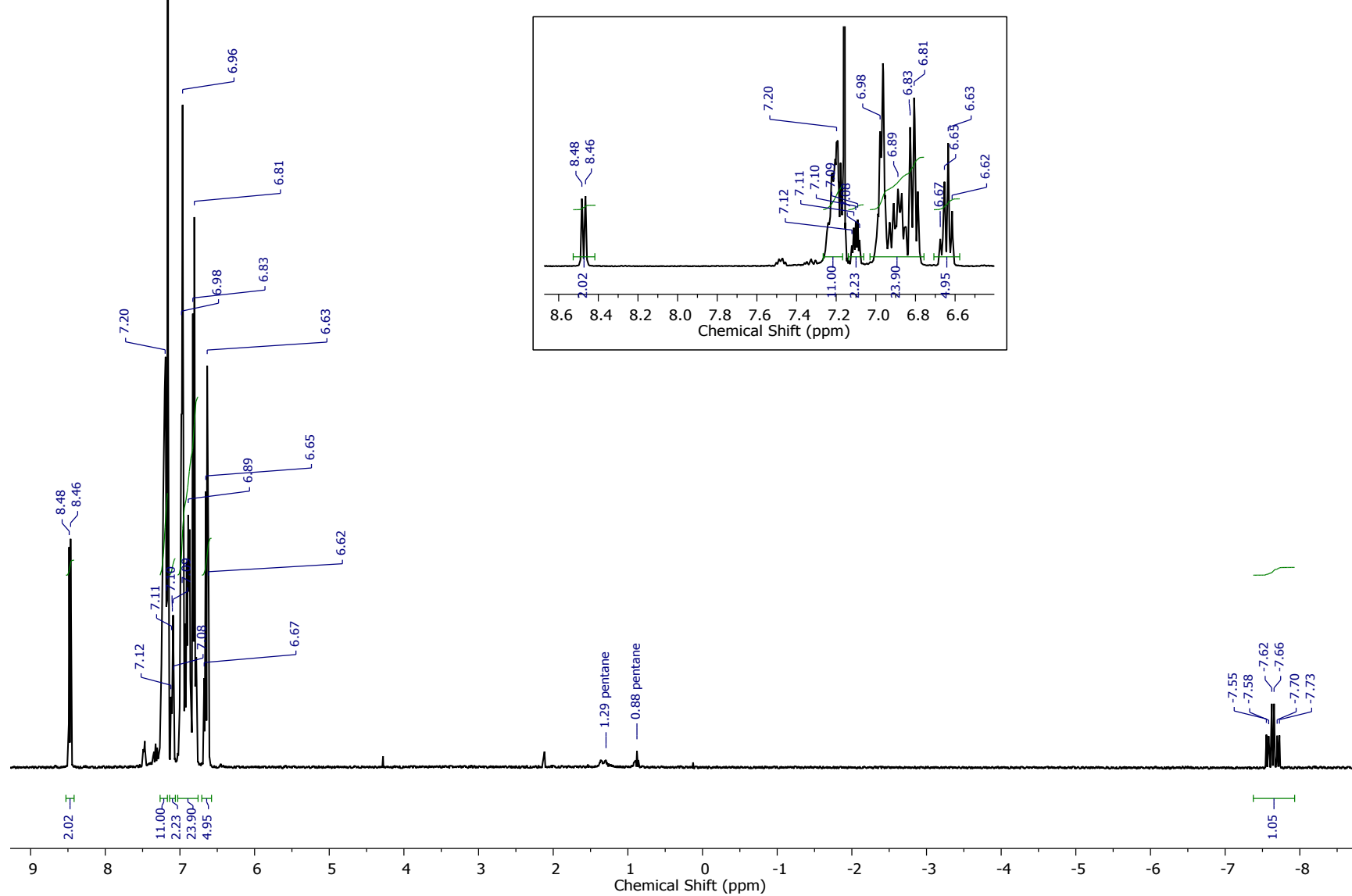


Figure S2. ¹H NMR spectrum of (^{Ph}P₂SiH)Ru(H)(CO)(PPh₃) (**2**) in C₆D₆

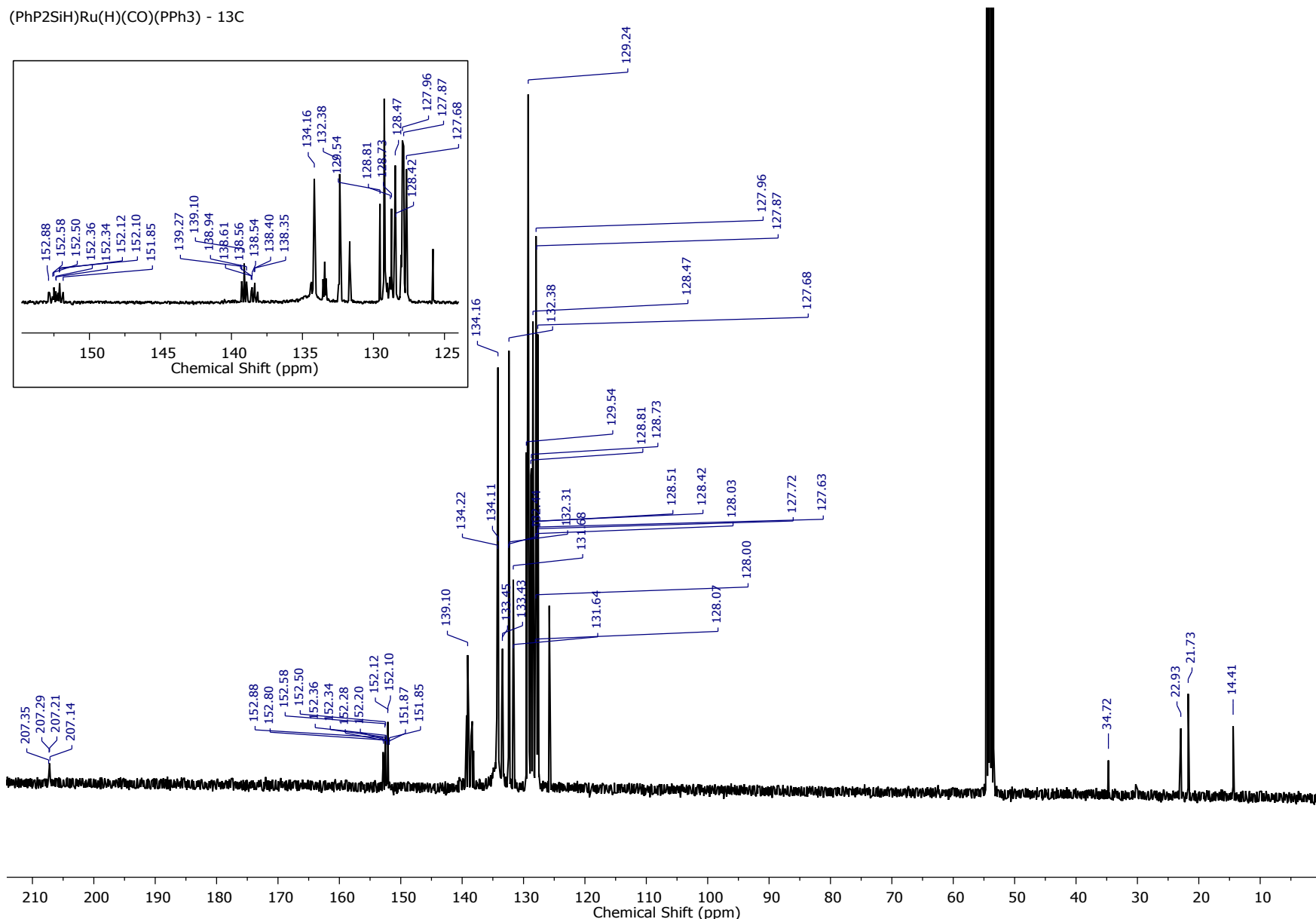


Figure S3. ¹³C{¹H} NMR spectrum of (PhP₂SiH)Ru(H)(CO)(PPh₃) (**2**) in CD₂Cl₂

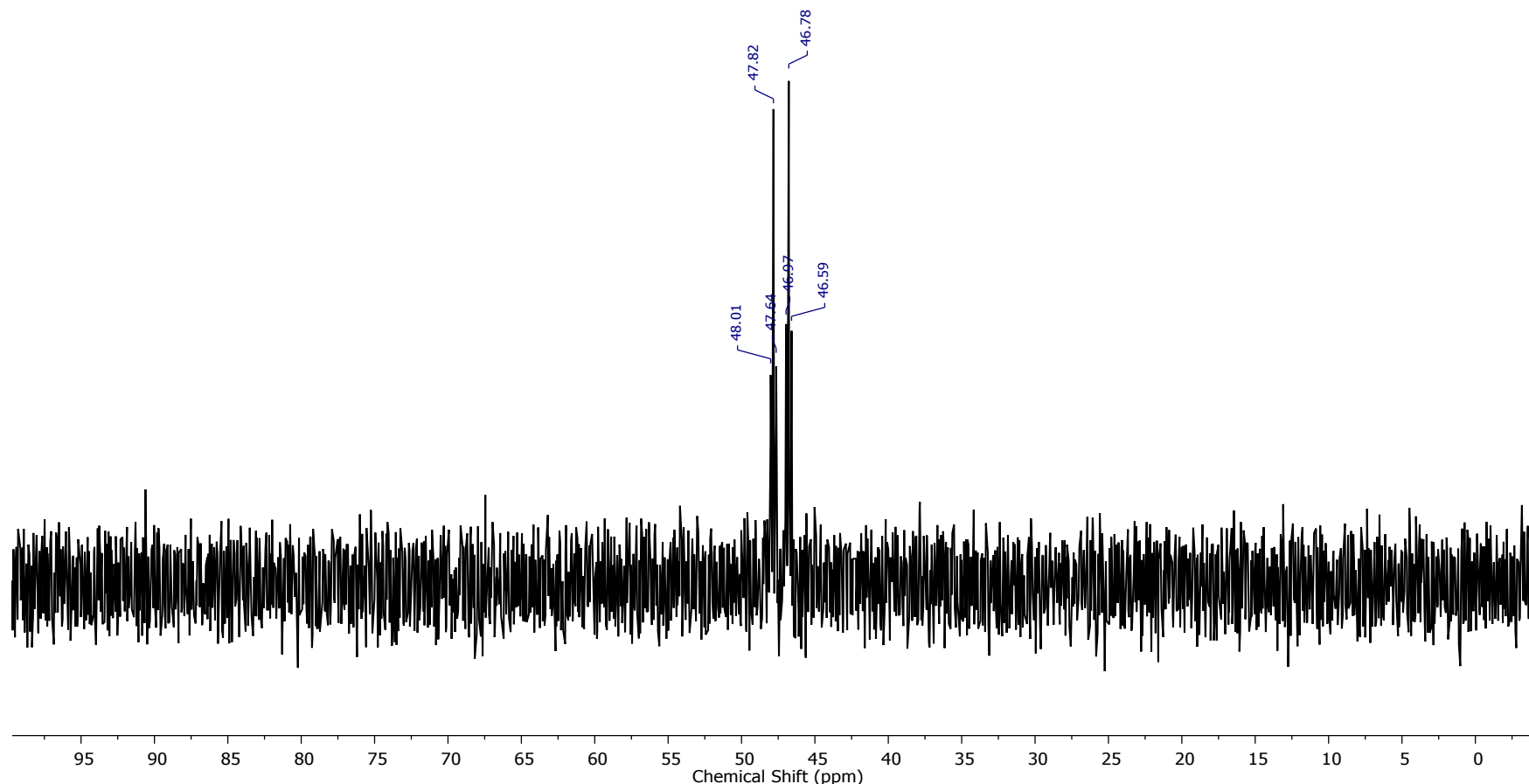


Figure S4. $^{29}\text{Si}\{^1\text{H}\}$ NMR spectrum of $(^{\text{Ph}}\text{P}_2\text{Si}^{\text{H}})\text{Ru}(\text{H})(\text{CO})(\text{PPh}_3)$ (**2**) in CH_2Cl_2

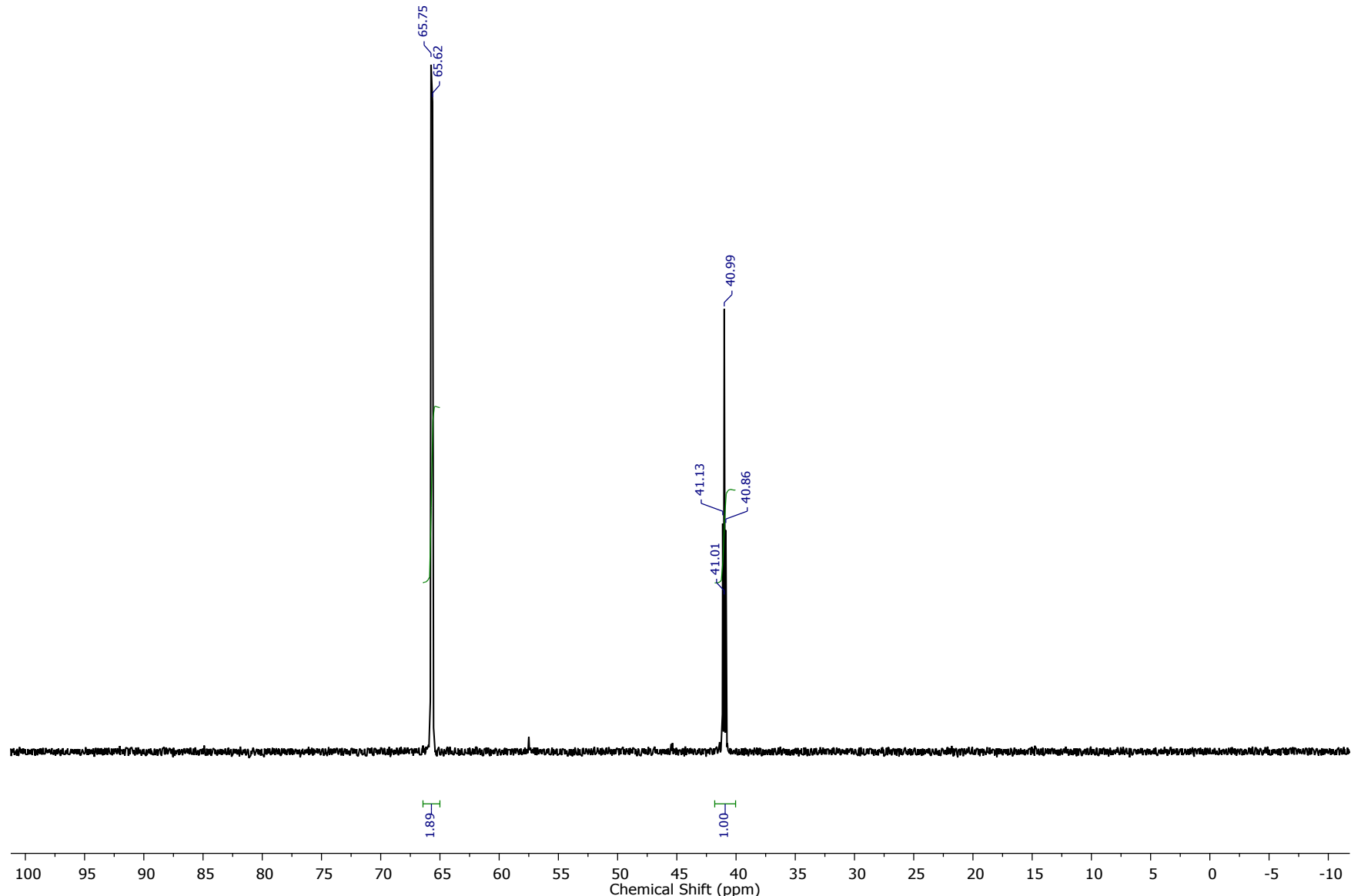


Figure S5. ³¹P{¹H} NMR spectrum of (PhP₂SiH)Ru(H)(CO)(PPh₃) (**2**) in CH_2Cl_2

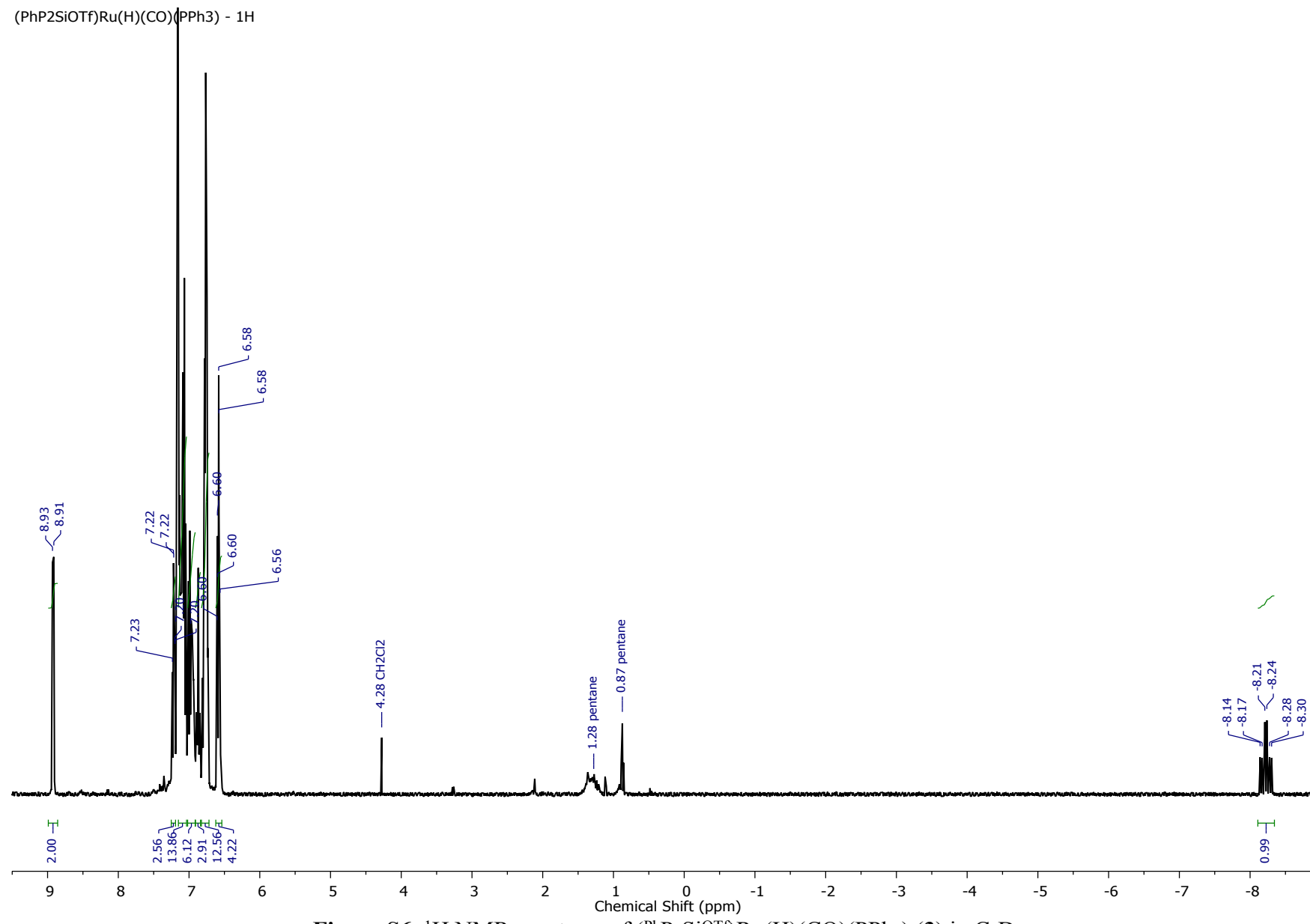


Figure S6. ^1H NMR spectrum of $(^{\text{Ph}}\text{P}_2\text{Si}^{\text{OTf}})\text{Ru}(\text{H})(\text{CO})(\text{PPh}_3)$ (**3**) in C_6D_6

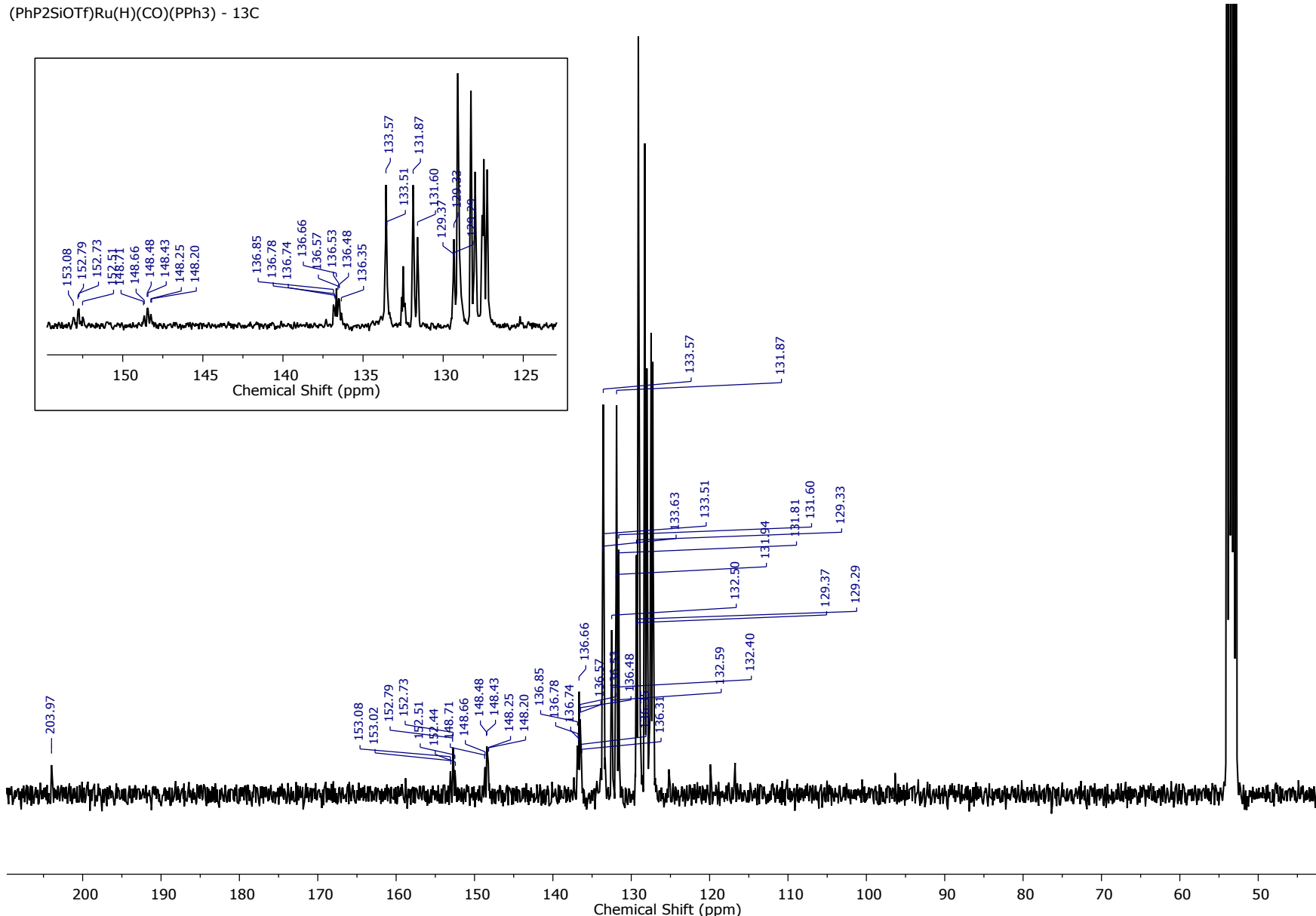


Figure S7. ¹³C{¹H} NMR spectrum of (^{PhP₂SiOTf})Ru(H)(CO)(PPh₃) (**3**) in CD₂Cl₂

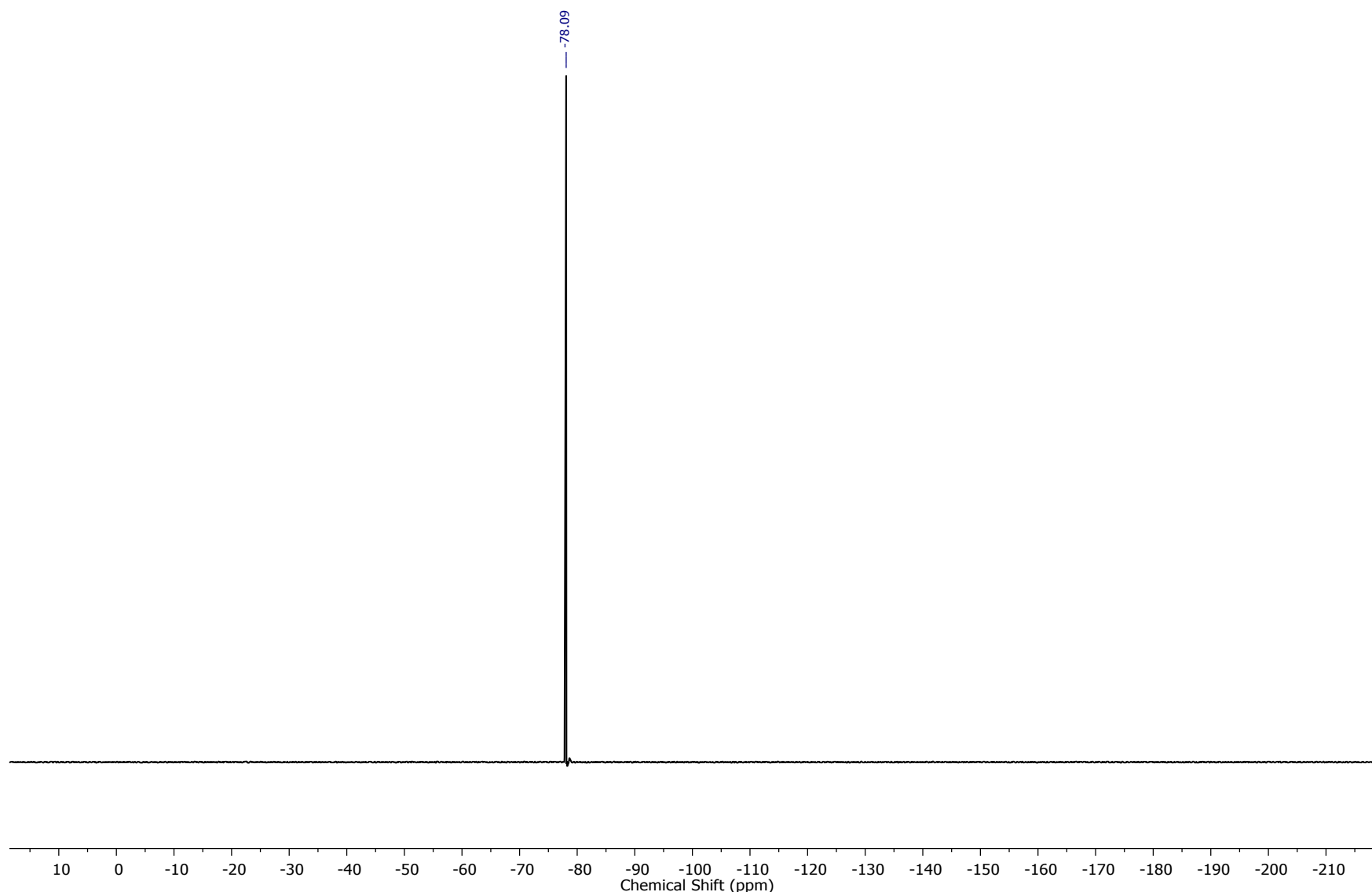


Figure S8. ¹⁹F{¹H} NMR spectrum of (PhP₂SiOTf)Ru(H)(CO)(PPh₃) (**3**) in CH₂Cl₂

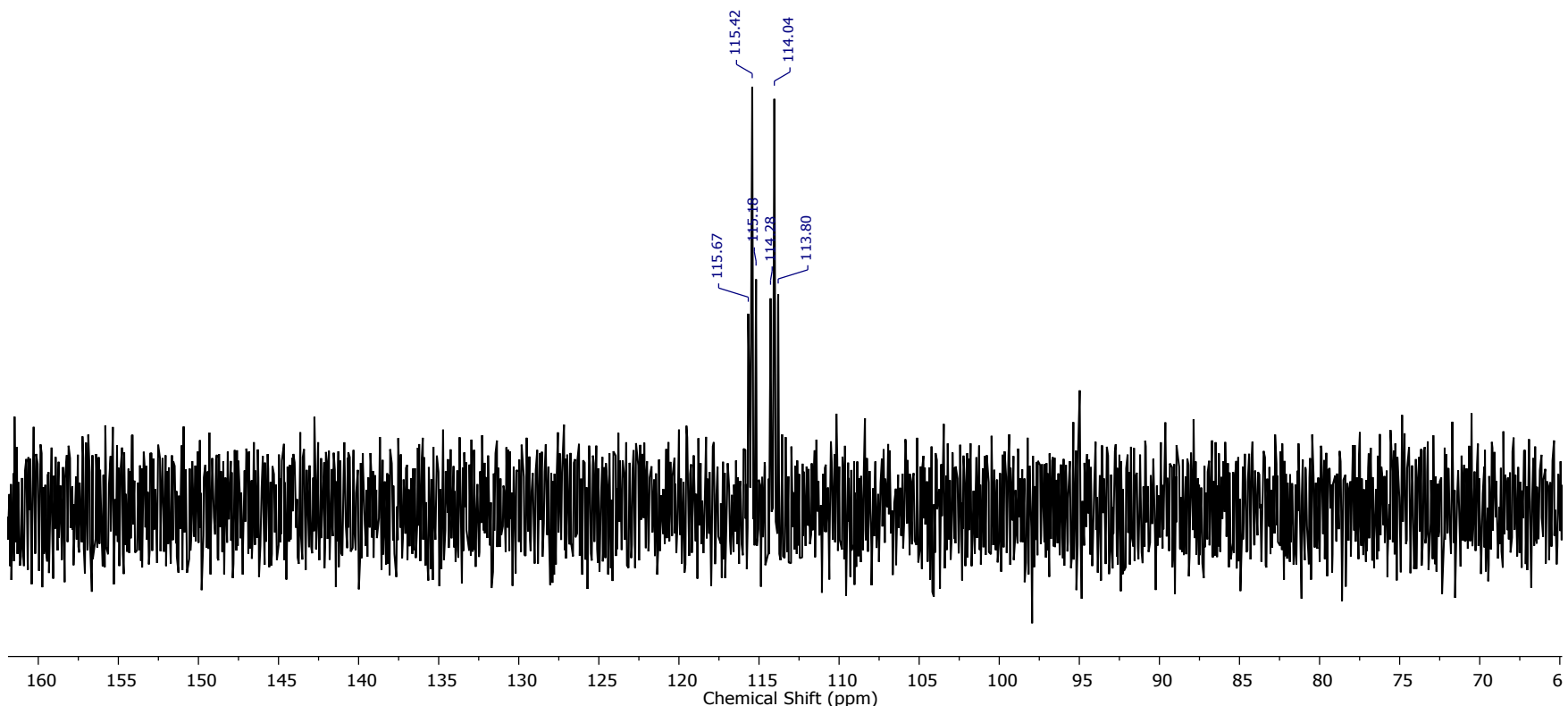


Figure S9. ²⁹Si{¹H} NMR spectrum of (PhP₂SiOTf)Ru(H)(CO)(PPh₃) (**3**) in CH₂Cl₂

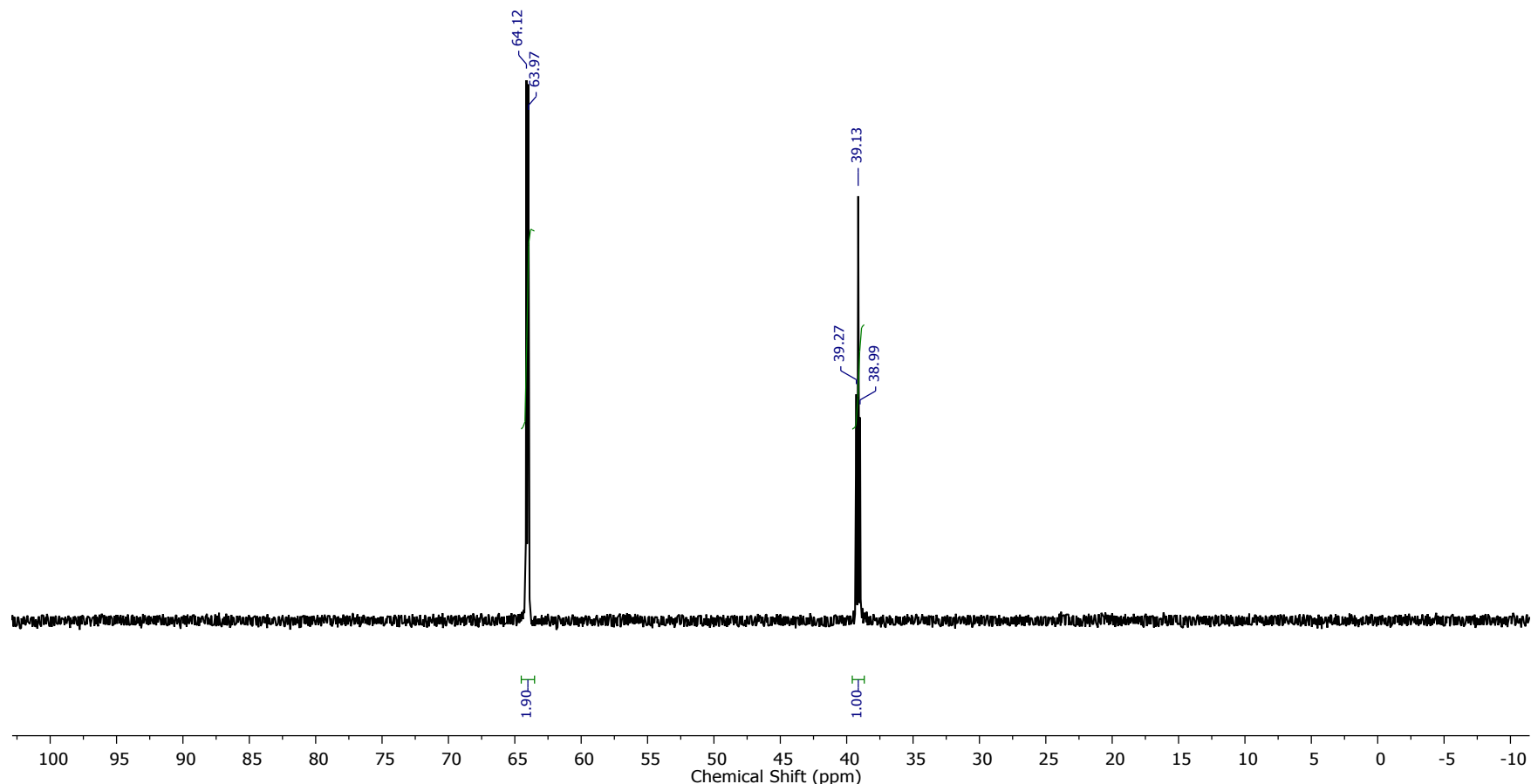


Figure S10. ³¹P{¹H} NMR spectrum of (PhP₂SiOTf)Ru(H)(CO)(PPh₃) (**3**) in CH₂Cl₂

$[(\text{PhP}_2\text{SiOEt}_2)\text{Ru}(\text{H})(\text{CO})(\text{PPh}_3)][\text{BArF}] - 1\text{H}$

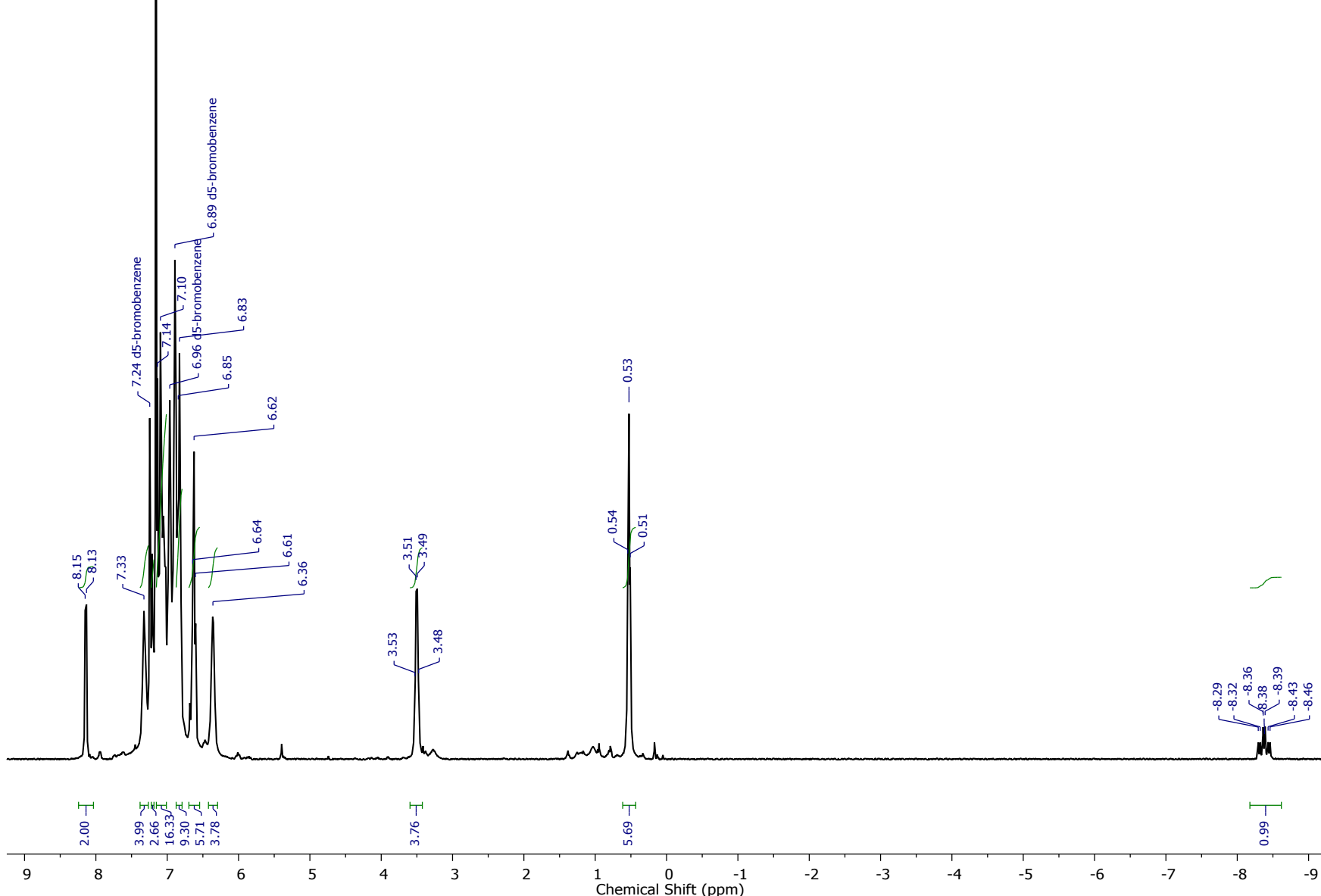


Figure S11. ${}^1\text{H}$ NMR spectrum of $[(\text{PhP}_2\text{SiOEt}_2)\text{Ru}(\text{H})(\text{CO})(\text{PPh}_3)][\text{BArF}]$ (**4-BArF**) in $\text{C}_6\text{D}_6:\text{C}_6\text{D}_5\text{Br}$ [1:1]

$[(\text{PhP}_2\text{SiOEt}_2)\text{Ru}(\text{H})(\text{PPh}_3)(\text{CO})][\text{BArF}]$ - 29Si

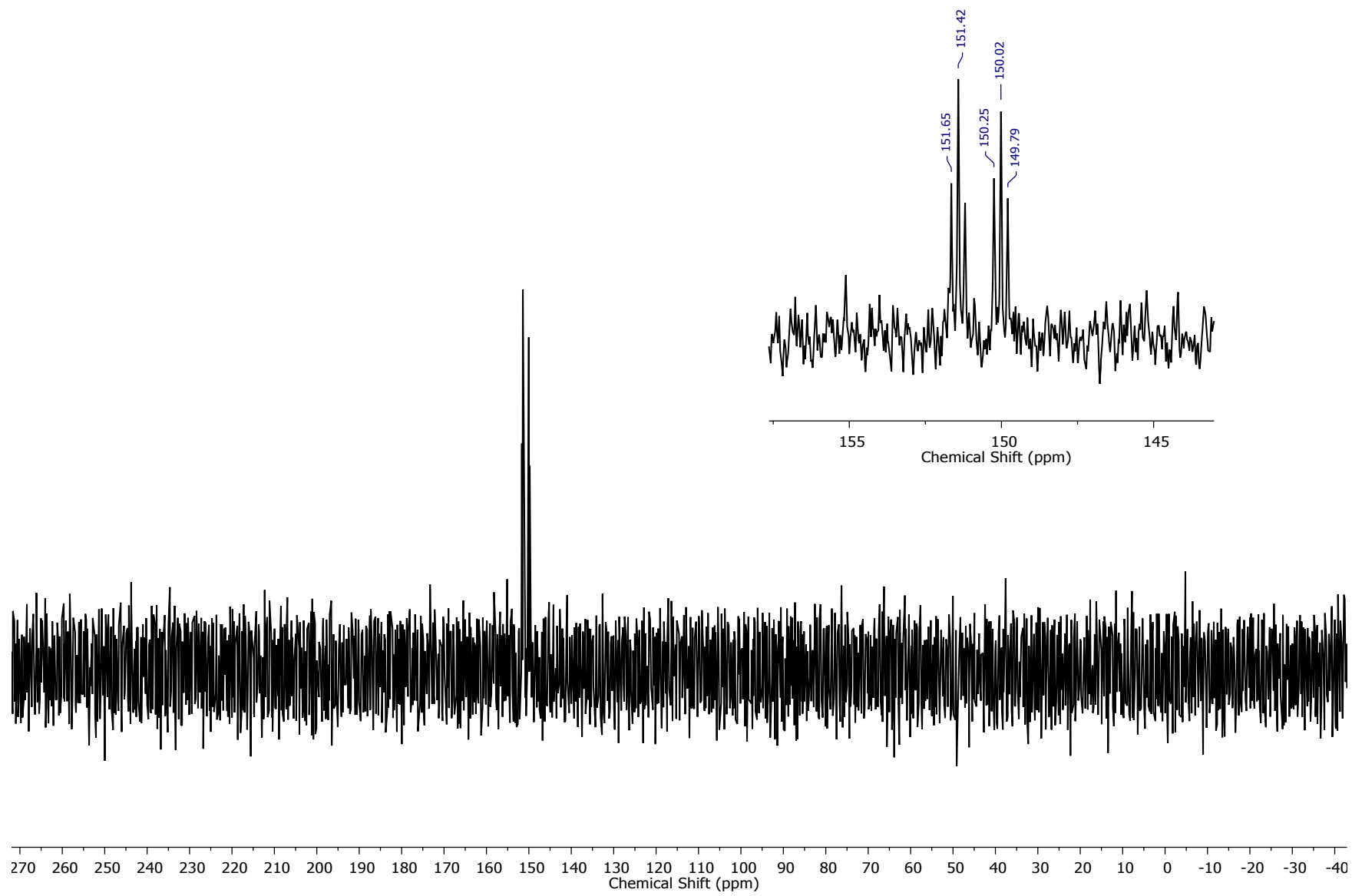


Figure S12. $^{29}\text{Si}\{^1\text{H}\}$ NMR spectrum of $[(\text{PhP}_2\text{SiOEt}_2)\text{Ru}(\text{H})(\text{CO})(\text{PPh}_3)][\text{BArF}]$ (**4-BArF**) in $\text{C}_6\text{H}_5\text{F}$

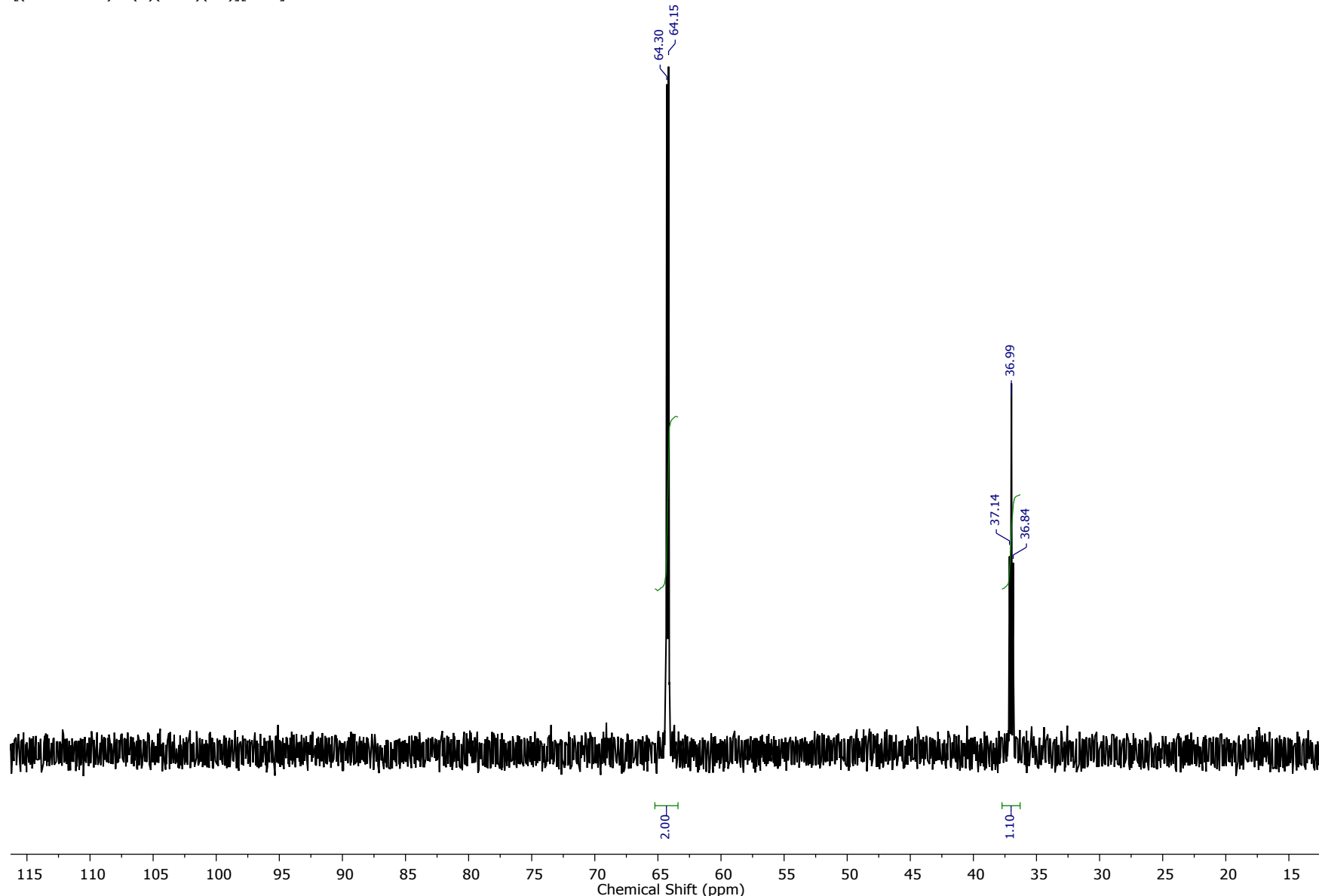


Figure S13. $^{31}\text{P}\{^1\text{H}\}$ NMR spectrum of $[(\text{PhP}_2\text{SiOEt}_2)\text{Ru}(\text{H})(\text{CO})(\text{PPh}_3)][\text{BArF}]$ (4-BArF) in $\text{C}_6\text{H}_5\text{F}$

$[(\text{PhP}_2\text{Si}=\text{)}\text{Ru}(\text{H})(\text{CO})(\text{PPh}_3)]\text{[BArF]} - 1\text{H}$

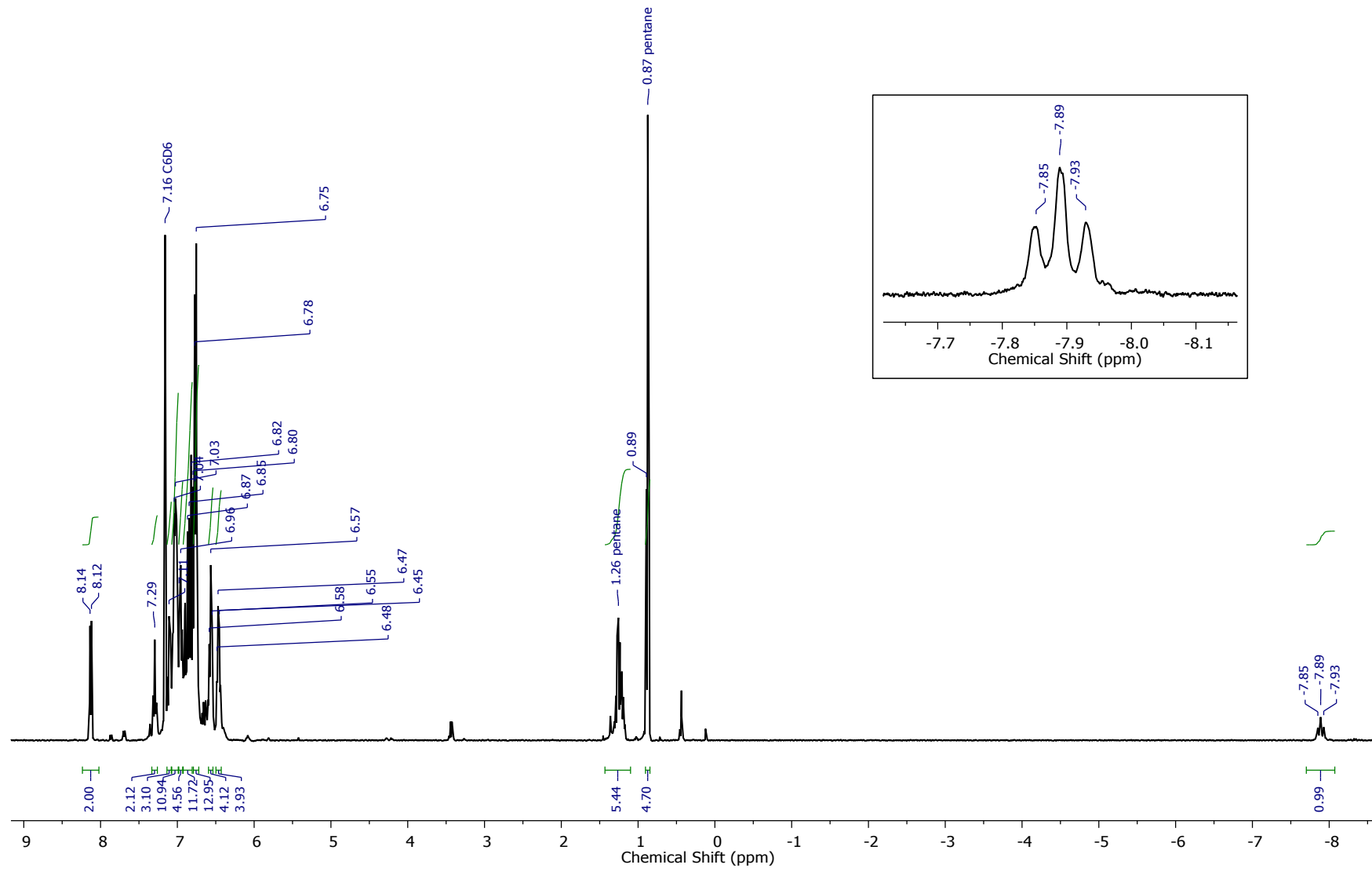


Figure S14. ^1H NMR spectrum of $[(\text{PhP}_2\text{Si}=\text{)}\text{Ru}(\text{H})(\text{CO})(\text{PPh}_3)]\text{[BArF]} - 1\text{H}$ (5-BArF) in C_6D_6

$[(\text{PhP}_2\text{Si}=\text{)}\text{Ru}(\text{H})(\text{CO})(\text{PPh}_3)]\text{[BArF]}$ - ${}^{29}\text{Si}$

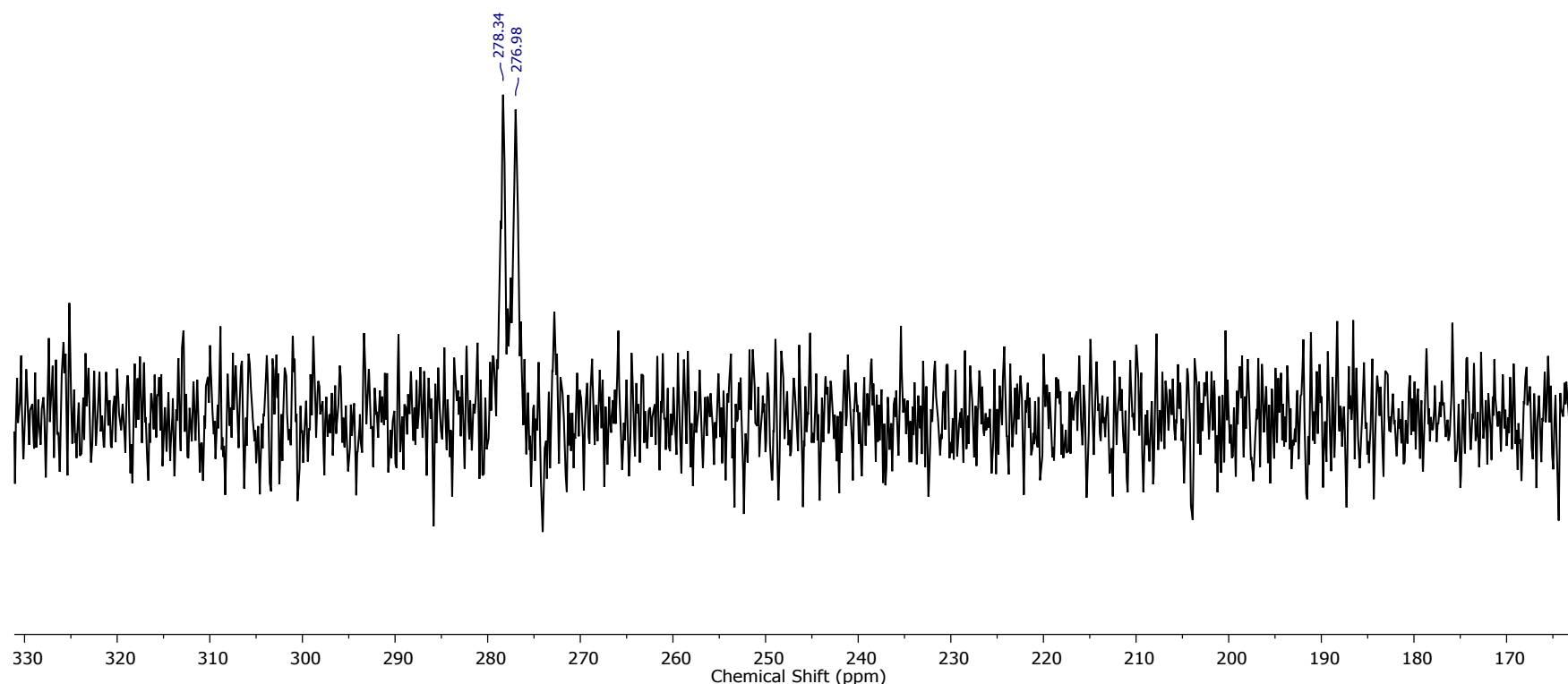


Figure S15. ${}^{29}\text{Si}\{{}^1\text{H}\}$ NMR spectrum of $[(\text{PhP}_2\text{Si}=\text{)}\text{Ru}(\text{H})(\text{CO})(\text{PPh}_3)]\text{[BArF]}$ (**5-BArF**) in $\text{C}_6\text{H}_5\text{F}$

$[(\text{PhP}_2\text{Si}=\text{)}\text{Ru}(\text{H})(\text{CO})(\text{PPh}_3)][\text{BArF}]$ - 31P

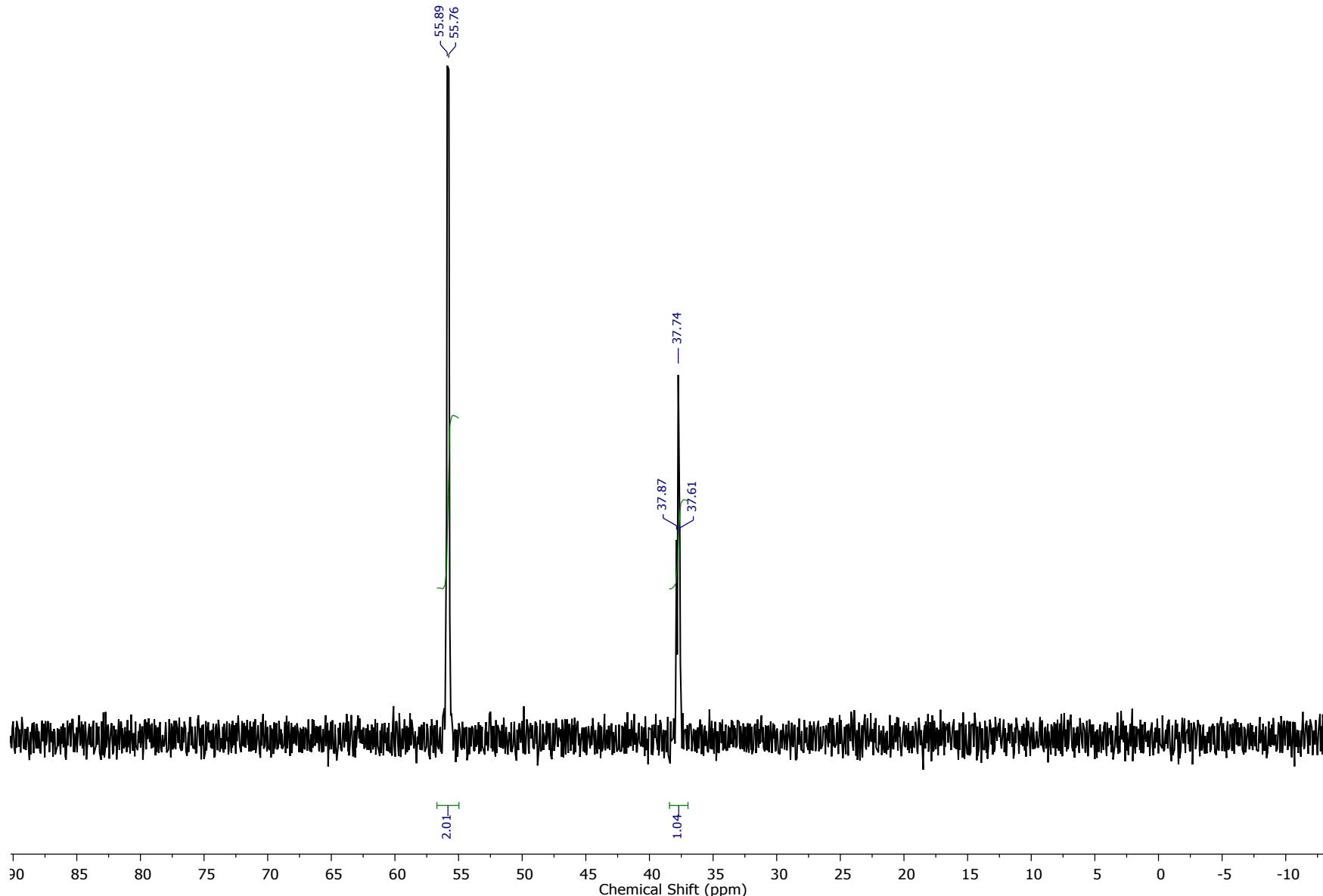


Figure S16. $^{31}\text{P}\{\text{H}\}$ NMR spectrum of $[(\text{PhP}_2\text{Si}=\text{)}\text{Ru}(\text{H})(\text{CO})(\text{PPh}_3)][\text{BArF}]$ (**5-BArF**) in $\text{C}_6\text{H}_5\text{F}$

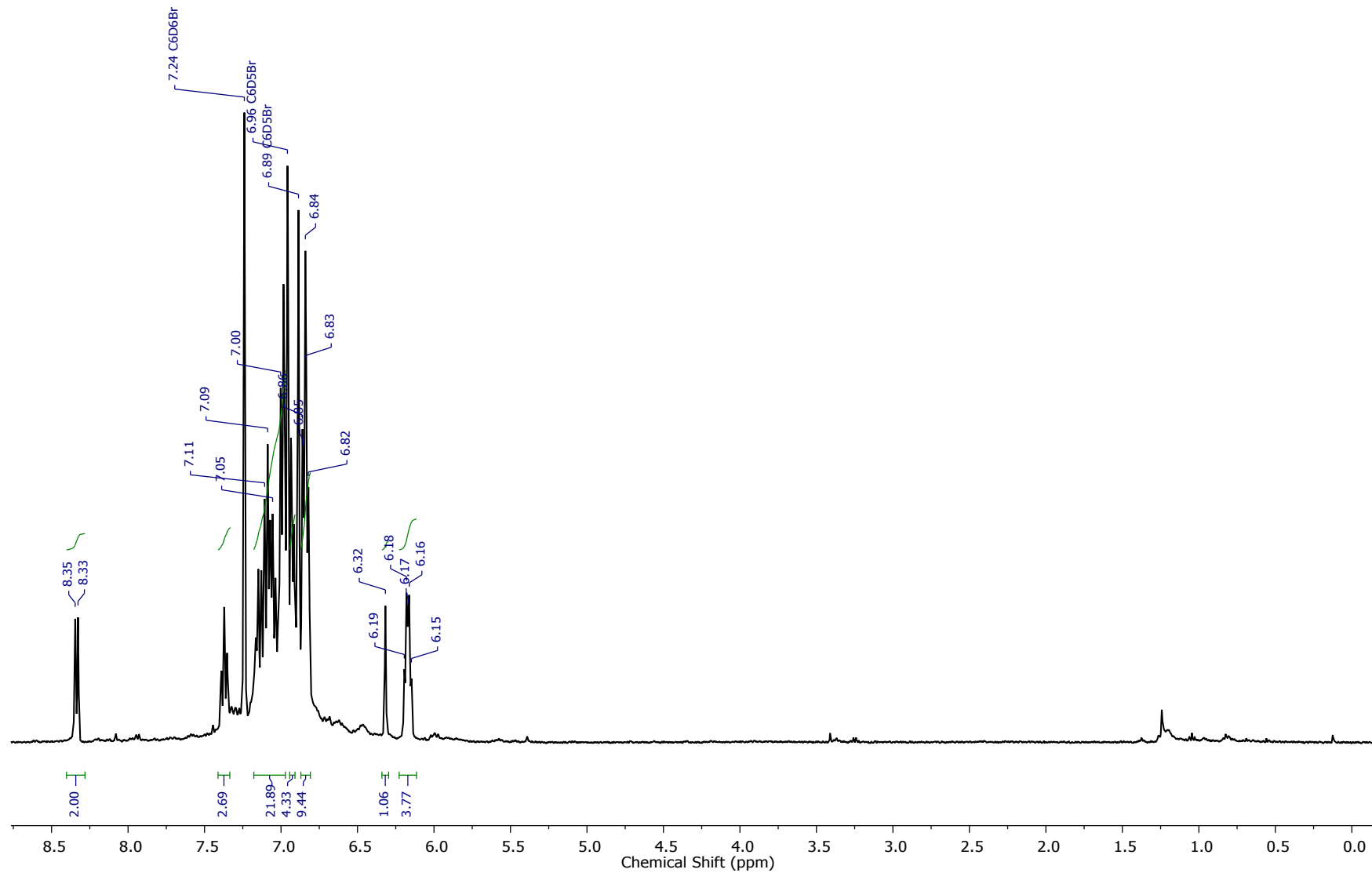


Figure S17. ^1H NMR spectrum of $[(\text{Ph}_2\text{PSiO}_2\text{CH})\text{Ru}(\text{CO})(\text{PPh}_3)][\text{BArF}]$ (**6-BArF**) in $\text{C}_6\text{D}_5\text{Br}$

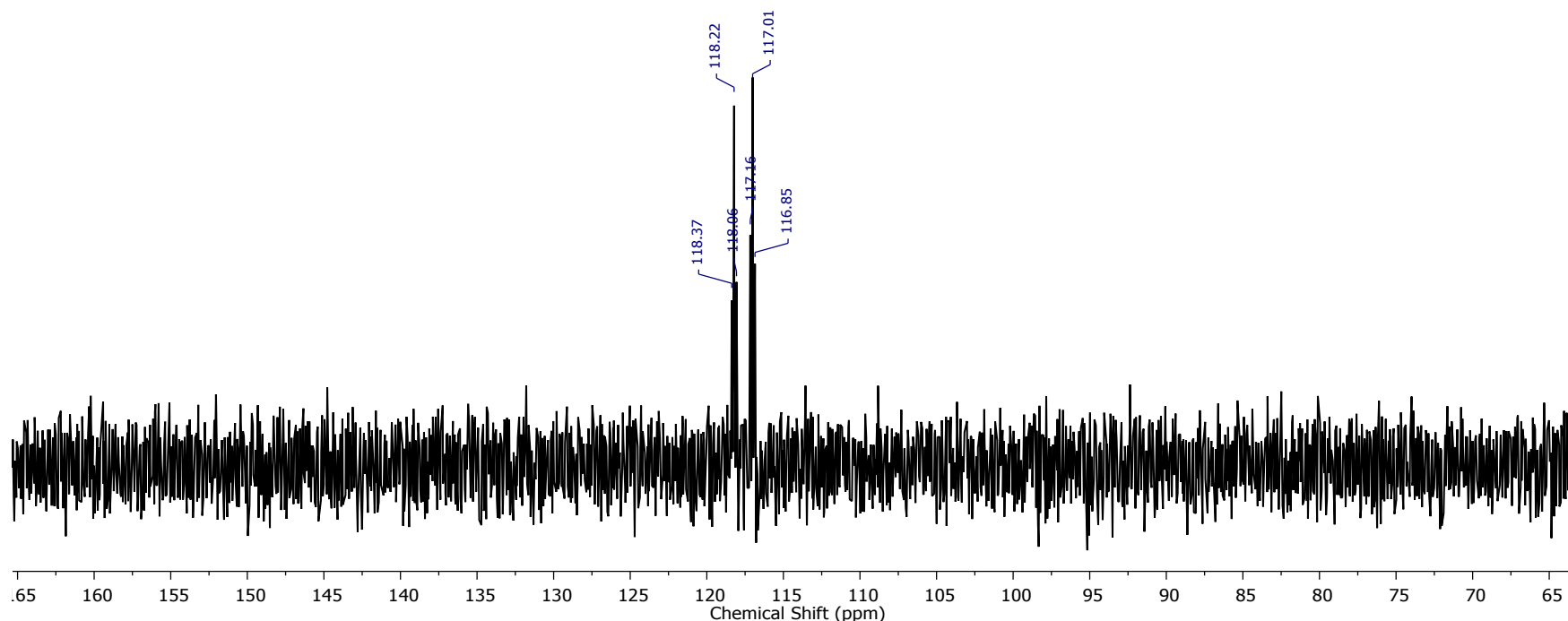


Figure S18. ²⁹Si{¹H} NMR spectrum of [(Ph₂PSiO₂CH)Ru(CO)(PPh₃)][BArF] (**6-BArF**) in C₆D₆:C₆H₅F [1:1]

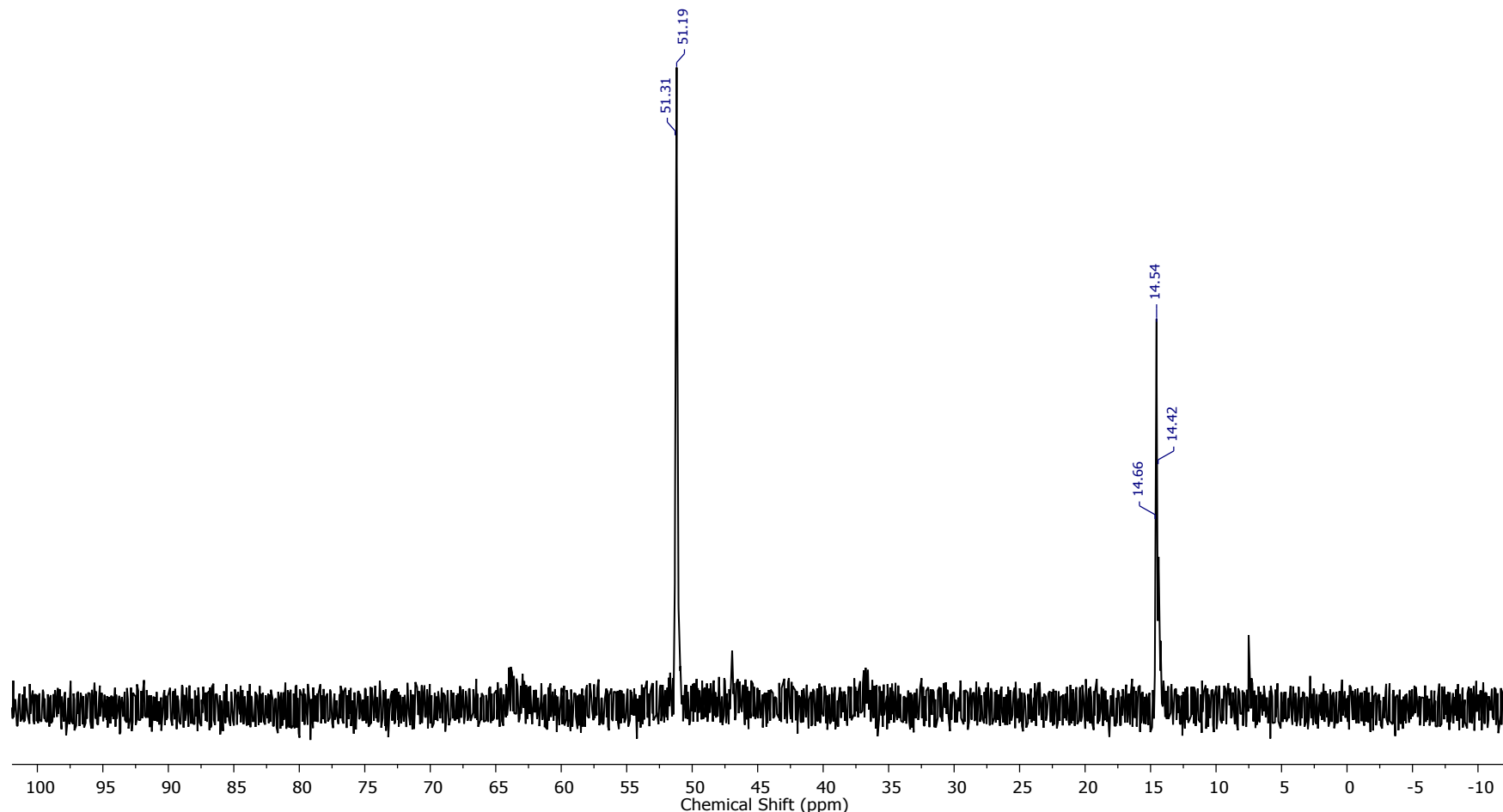


Figure S19. ³¹P{¹H} NMR spectrum of [(Ph₂PSiO₂CH)Ru(CO)(PPh₃)][BArF] (**6-BArF**) in C₆H₅F

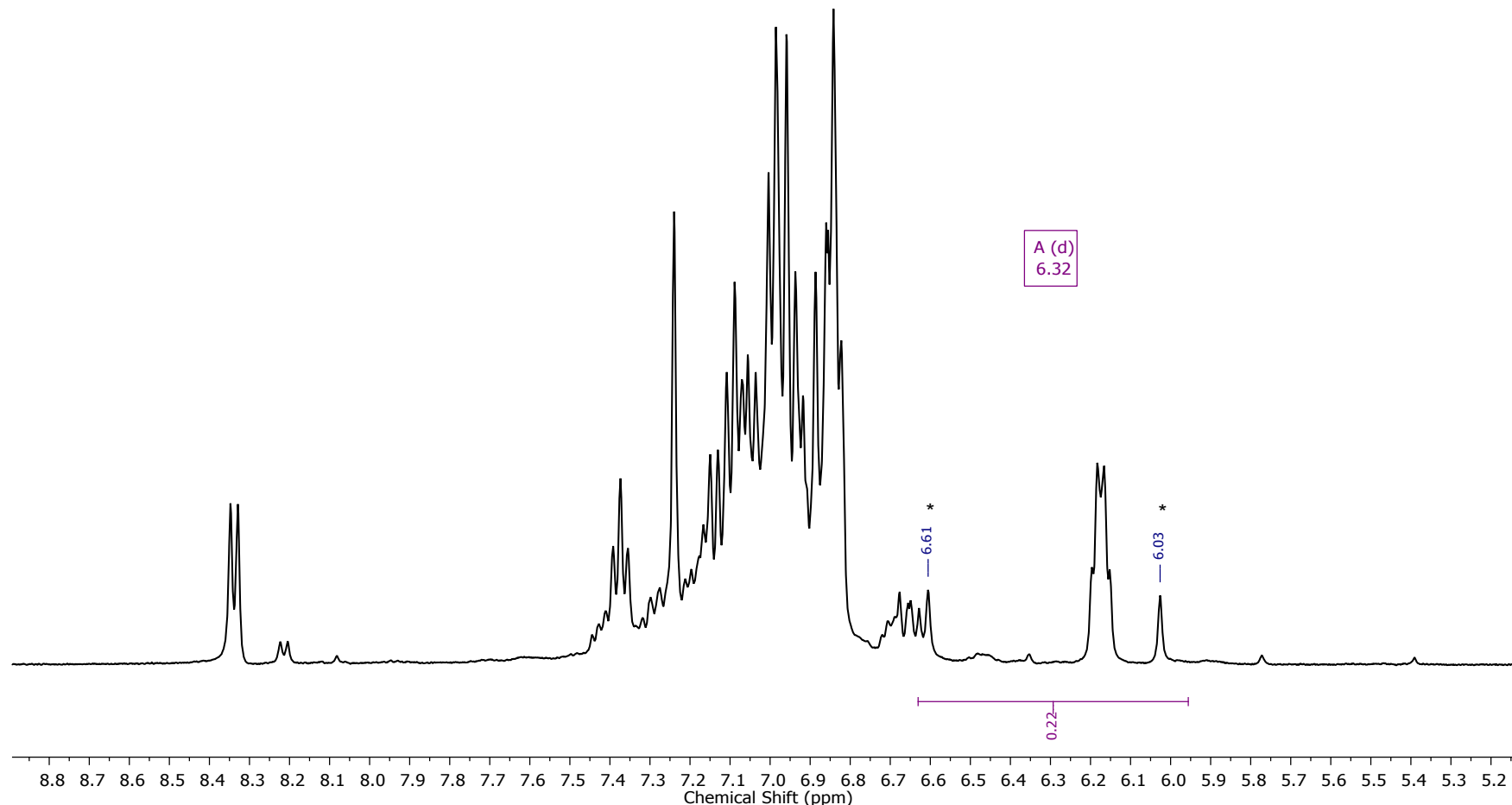


Figure S20. ¹H NMR spectrum of crude ¹³C-[($\text{PhP}_2\text{SiO}_2\text{CH})\text{Ru}(\text{CO})(\text{PPh}_3)\text{][BArF}$] (**6(¹³C)-BArF**) in $\text{C}_6\text{D}_5\text{Br}$.
The asterisks indicate components of the $H-\text{C}^{13}$ doublet.

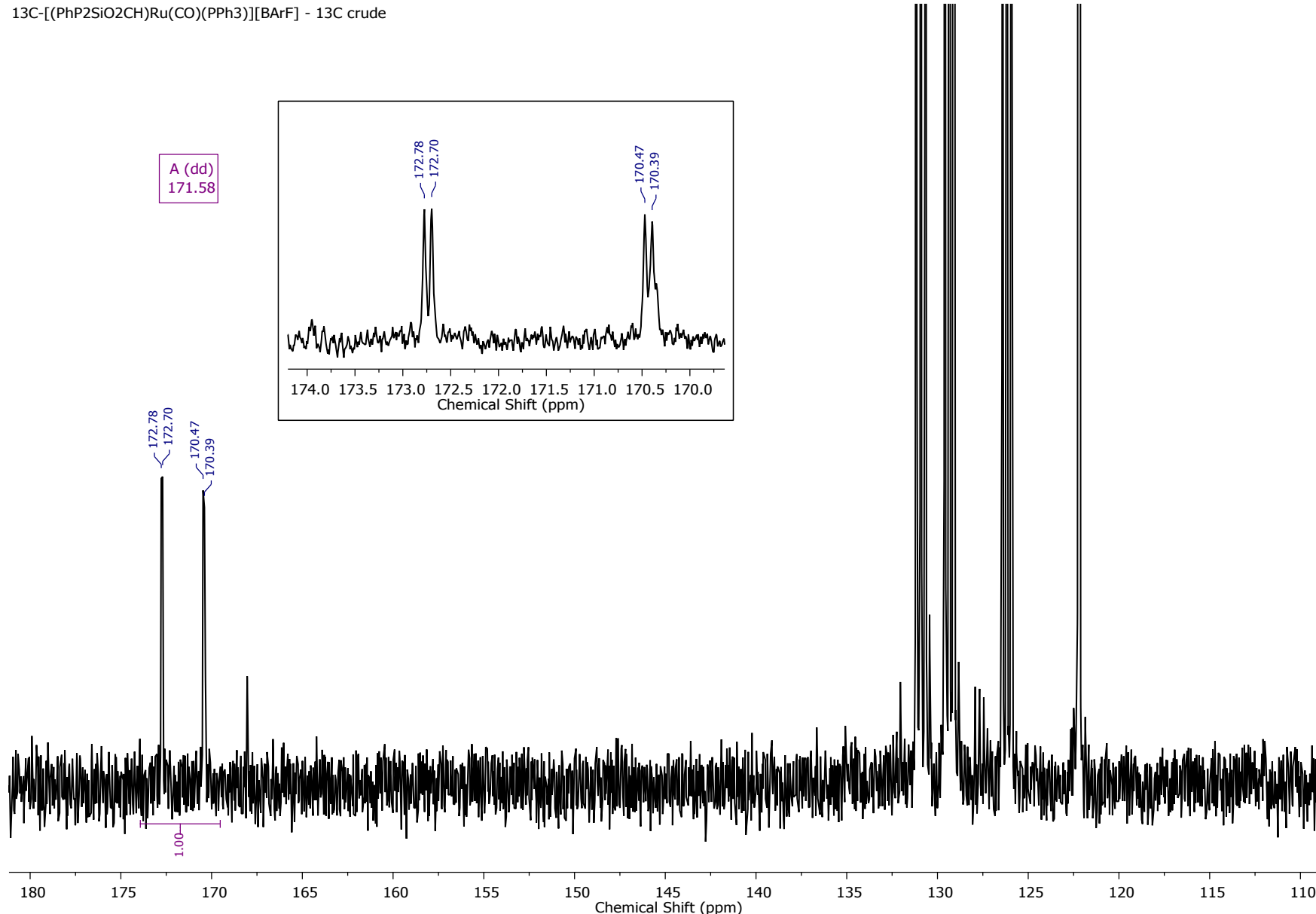


Figure S21. ^{13}C NMR spectrum of crude ^{13}C -[(PhP₂SiO₂CH)Ru(CO)(PPh₃)][BArF] (**6(¹³C)-BArF**) in C₆D₅Br, showing $^3\text{J}_{\text{CP}}$ and $^1\text{J}_{\text{CH}}$

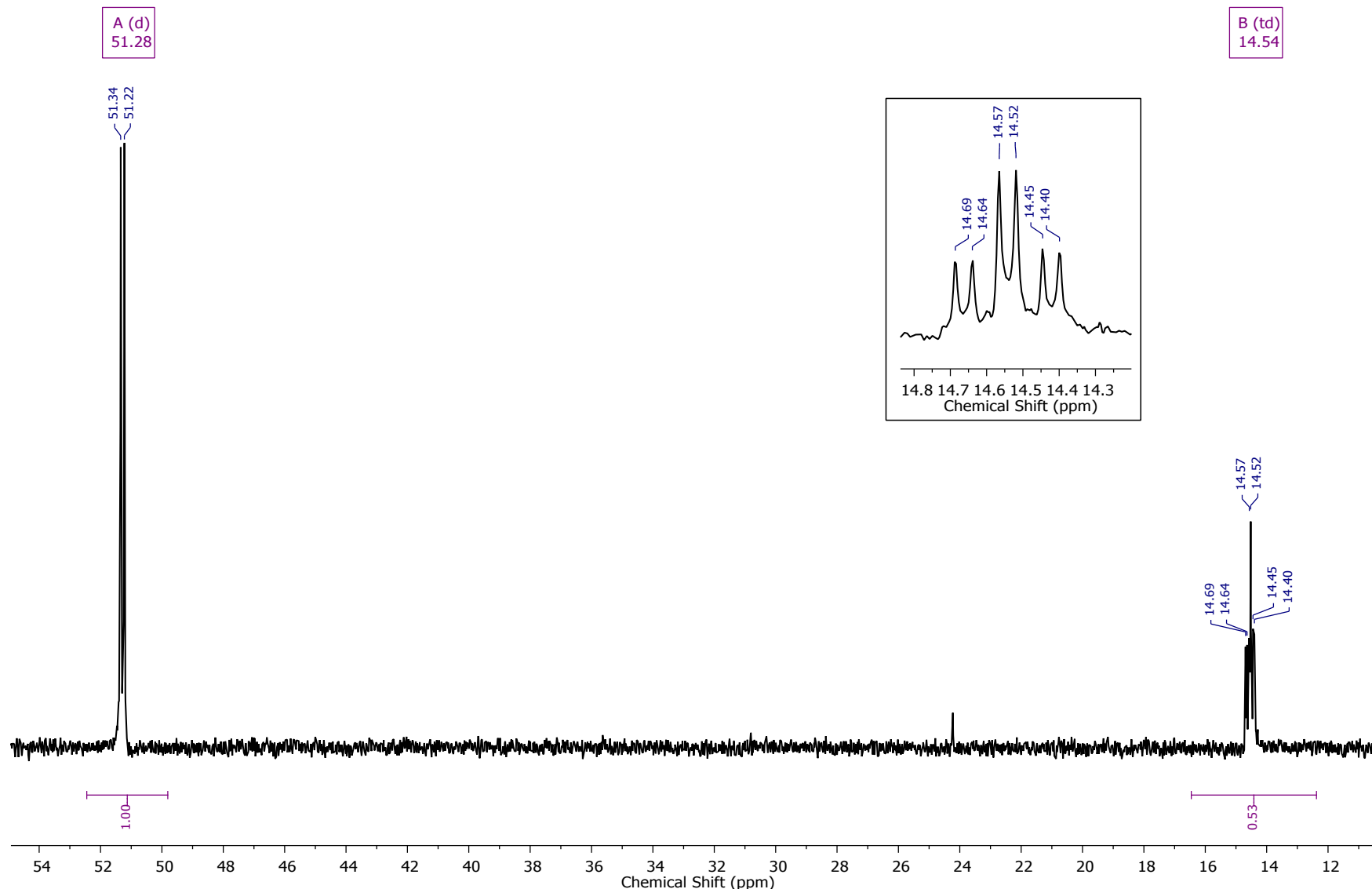


Figure S22. ^{31}P NMR spectrum of crude $^{13}\text{C}-[(\text{PhP}_2\text{SiO}_2\text{CH})\text{Ru}(\text{CO})(\text{PPh}_3)\text{][BArF}]$ (**6(¹³C)-BArF**) in $\text{C}_6\text{H}_5\text{F}$

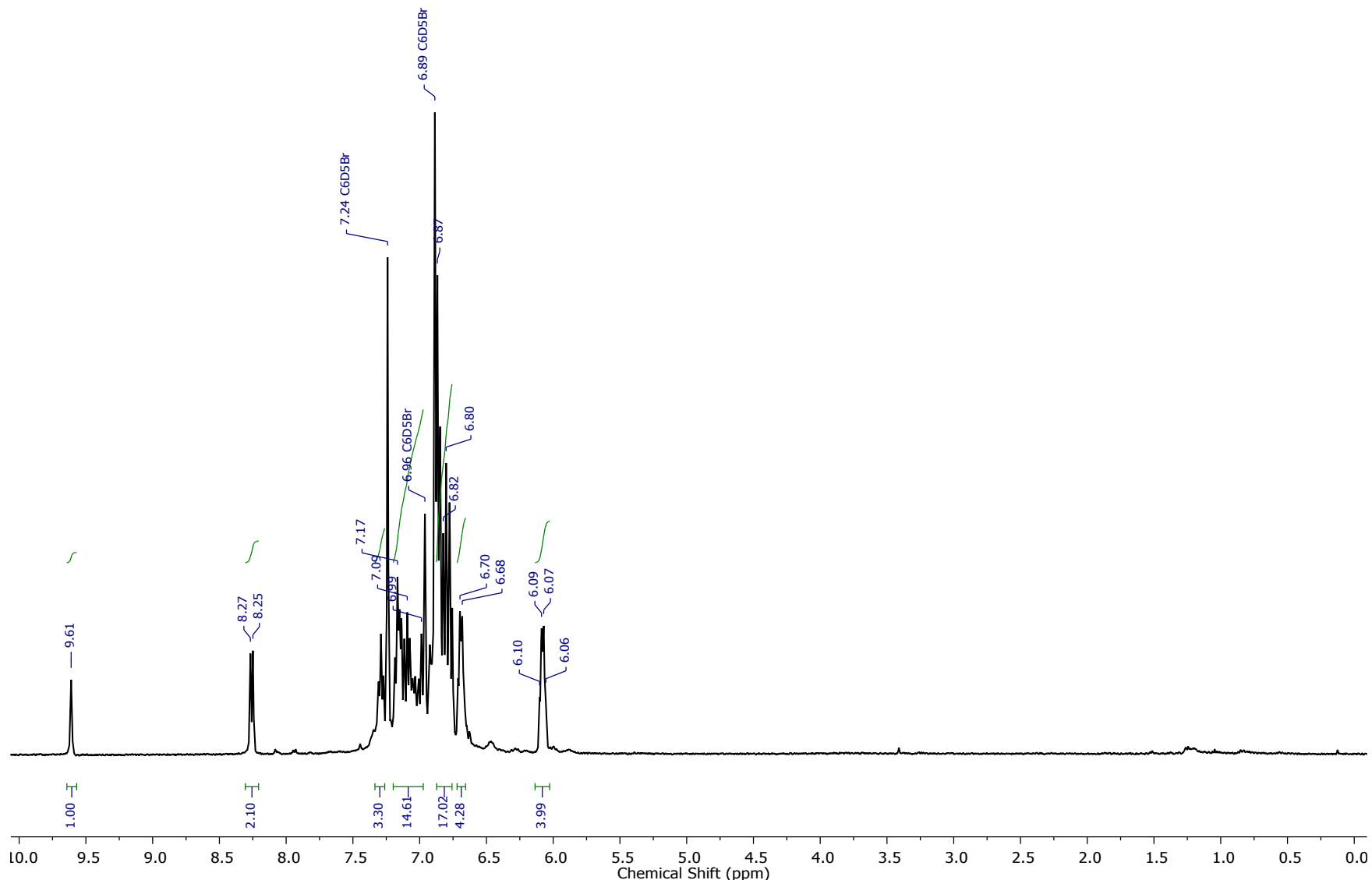


Figure S23. ^1H NMR spectrum of $[(\text{PhP}_2\text{Si}^{\text{S}2\text{CH}})\text{Ru}(\text{CO})(\text{PPh}_3)][\text{BArF}]$ (**7-BArF**) in $\text{C}_6\text{D}_5\text{Br}$

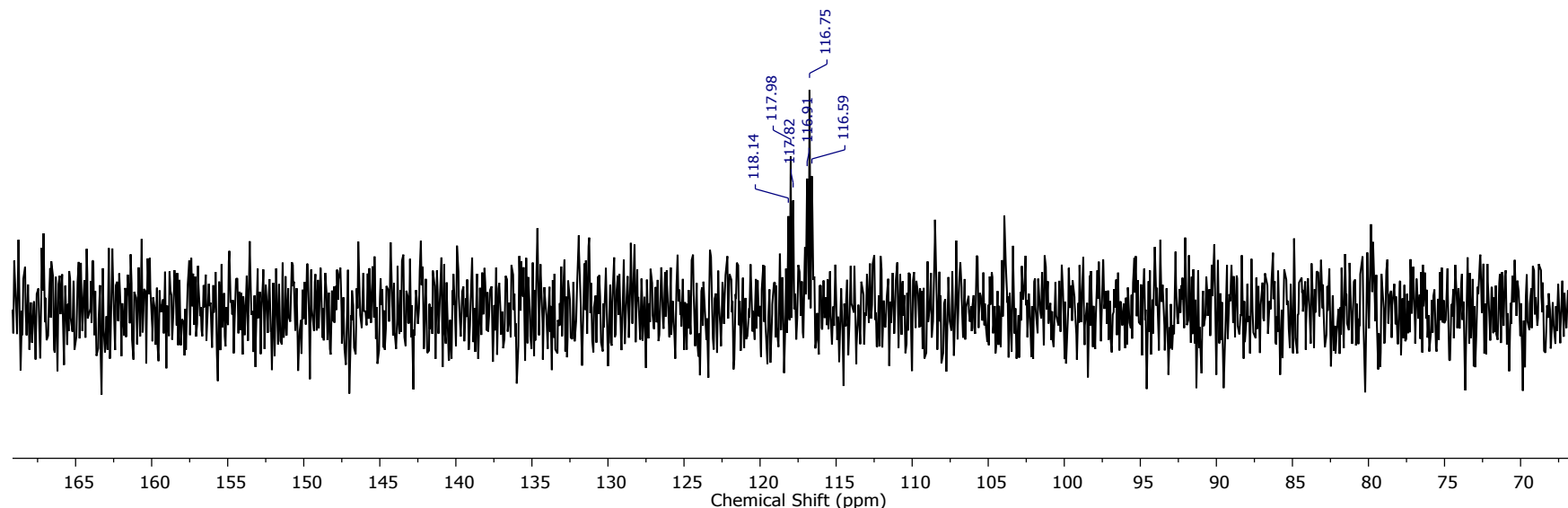


Figure S24. ^{29}Si NMR spectrum of $[(\text{PhP}_2\text{SiS}_2\text{CH})\text{Ru}(\text{CO})(\text{PPh}_3)][\text{BArF}]$ (7-BArF) in $\text{C}_6\text{D}_6:\text{C}_6\text{H}_5\text{F}$ [1:1]

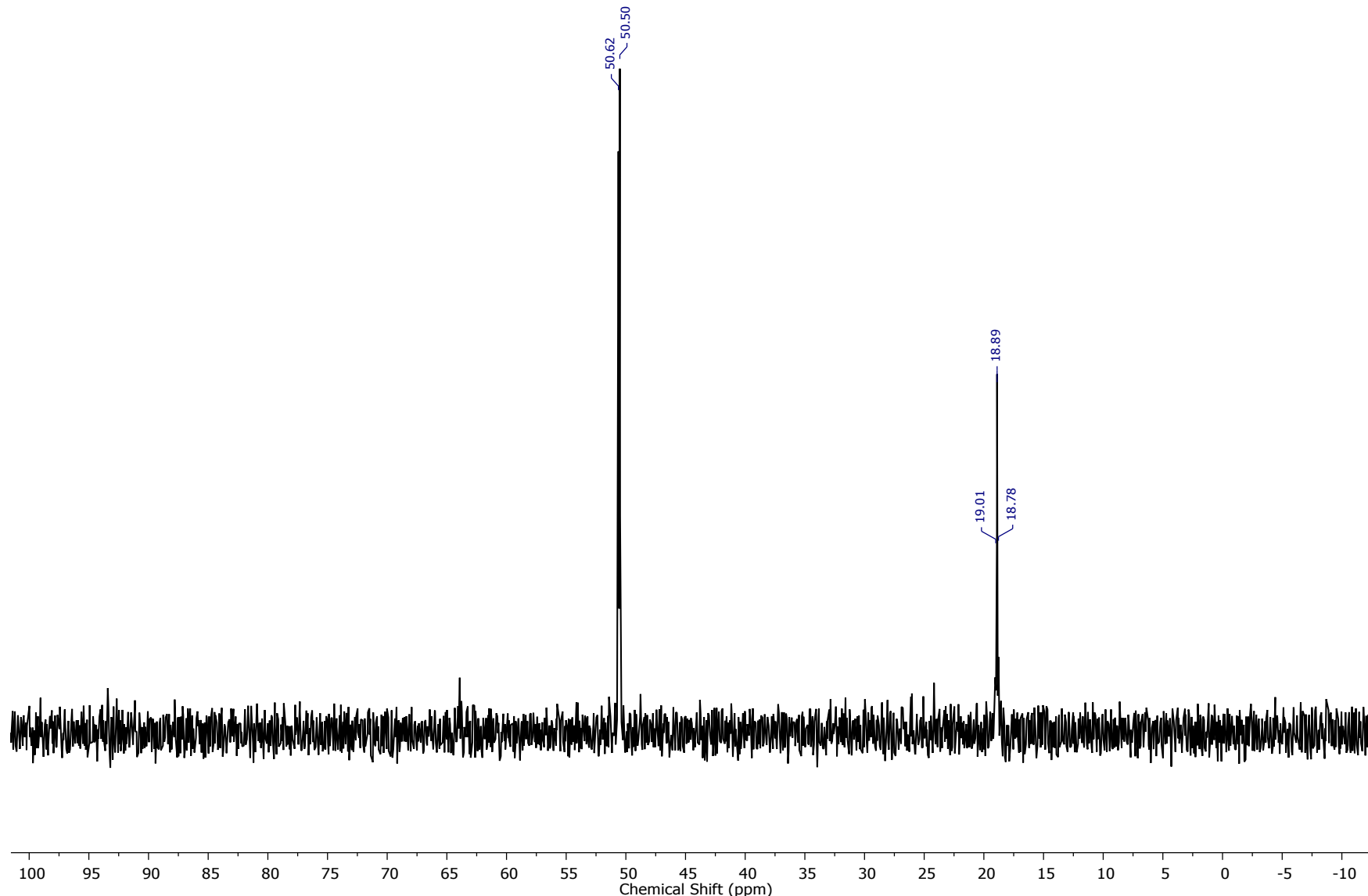


Figure S25. ^{31}P NMR spectrum of $[(\text{PhP}_2\text{SiS}^2\text{CH})\text{Ru}(\text{CO})(\text{PPh}_3)][\text{BArF}]$ (**7-BArF**) in $\text{C}_6\text{H}_5\text{F}$

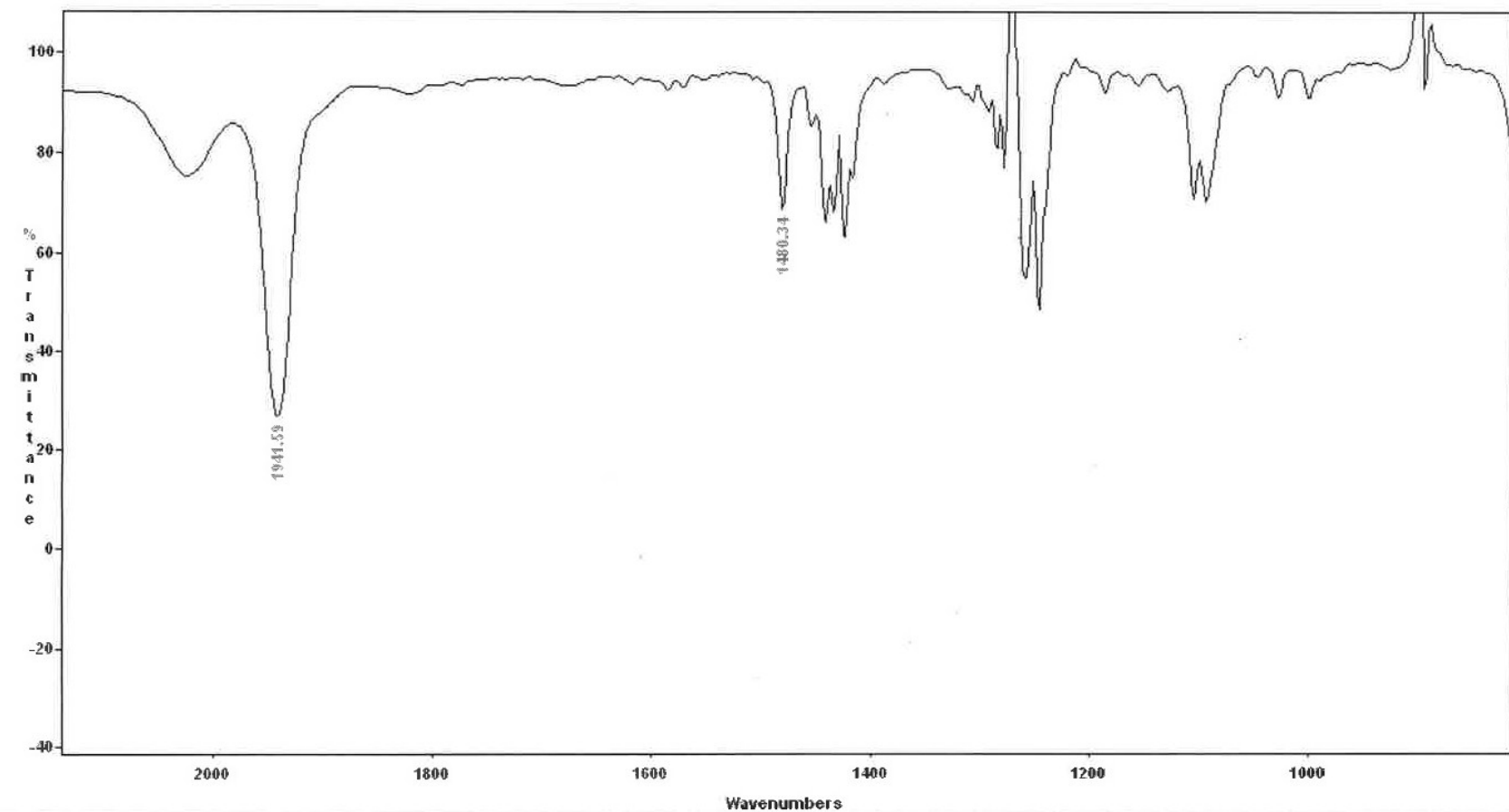


Figure S26. Infrared spectrum of $(^{Ph}P_2Si^H)Ru(H)(CO)(PPh_3)$ in CH_2Cl_2

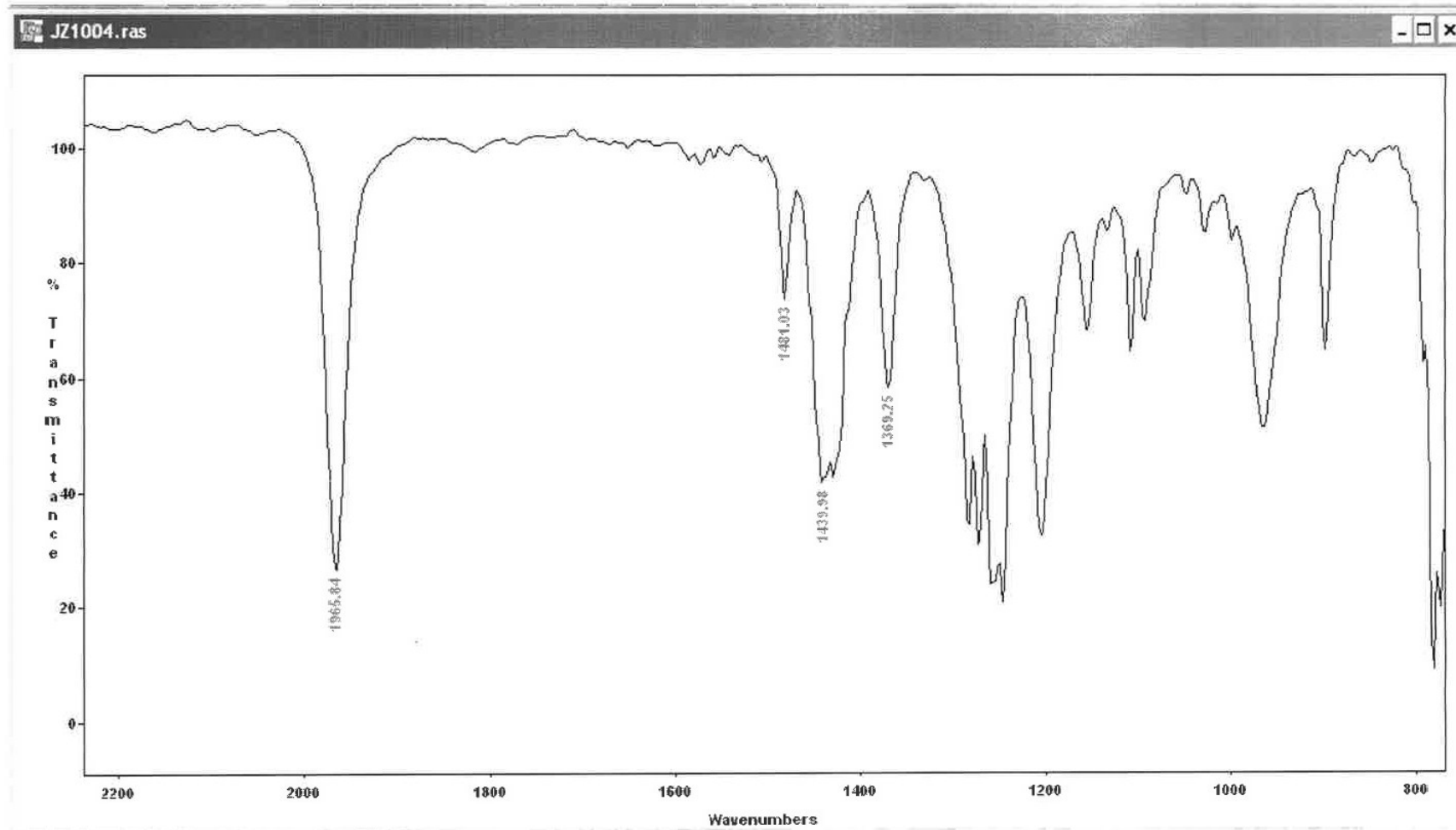


Figure S27. Infrared spectrum of $(^{Ph}P_2Si^{OTf})Ru(H)(CO)(PPh_3)$ in CH_2Cl_2

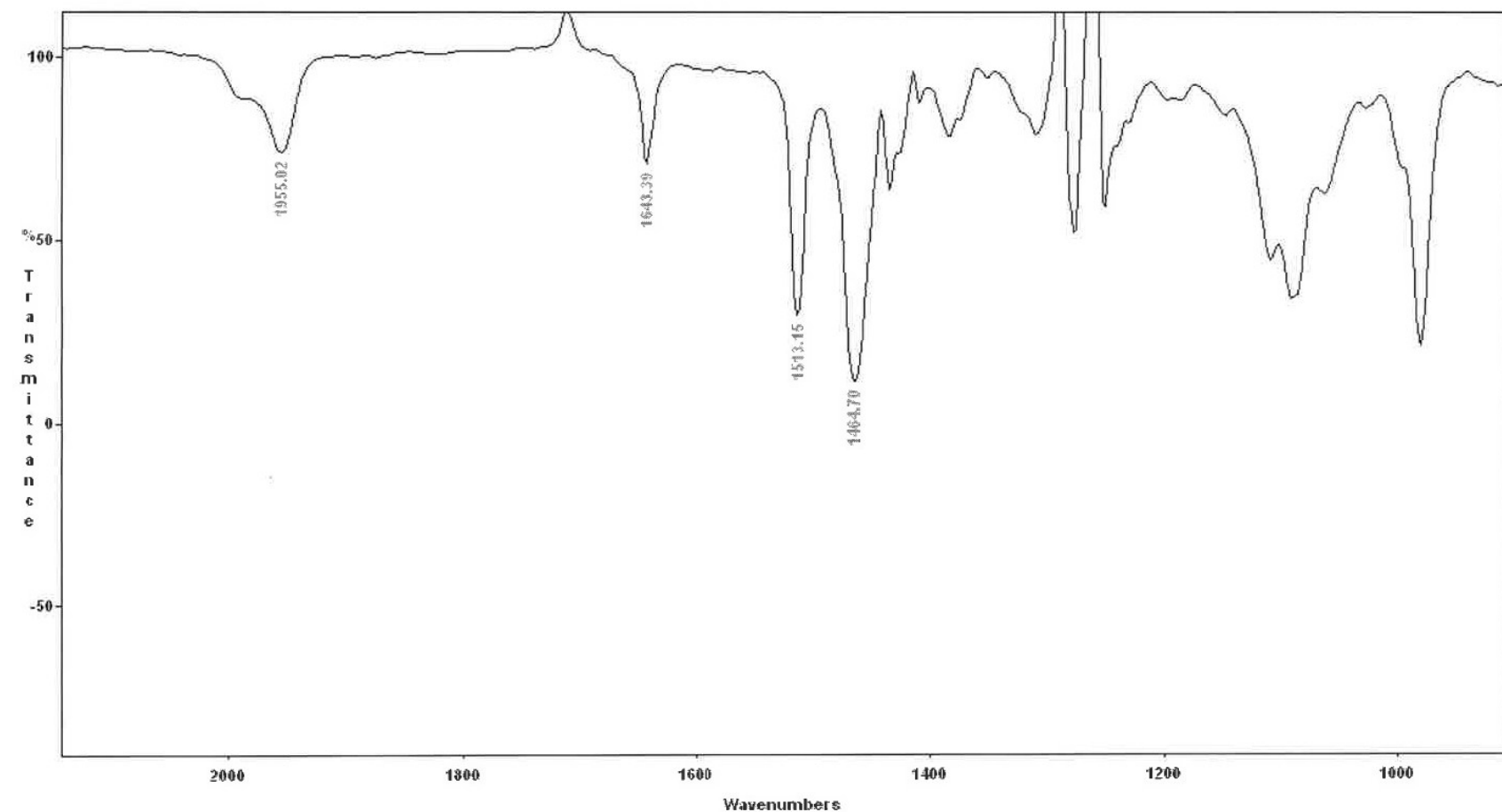


Figure S28. Infrared spectrum of $[(^{\text{Ph}}\text{P}_2\text{Si}^{\text{OEt}2})\text{Ru}(\text{H})(\text{CO})(\text{PPh}_3)][\text{BArF}]$ in CH_2Cl_2

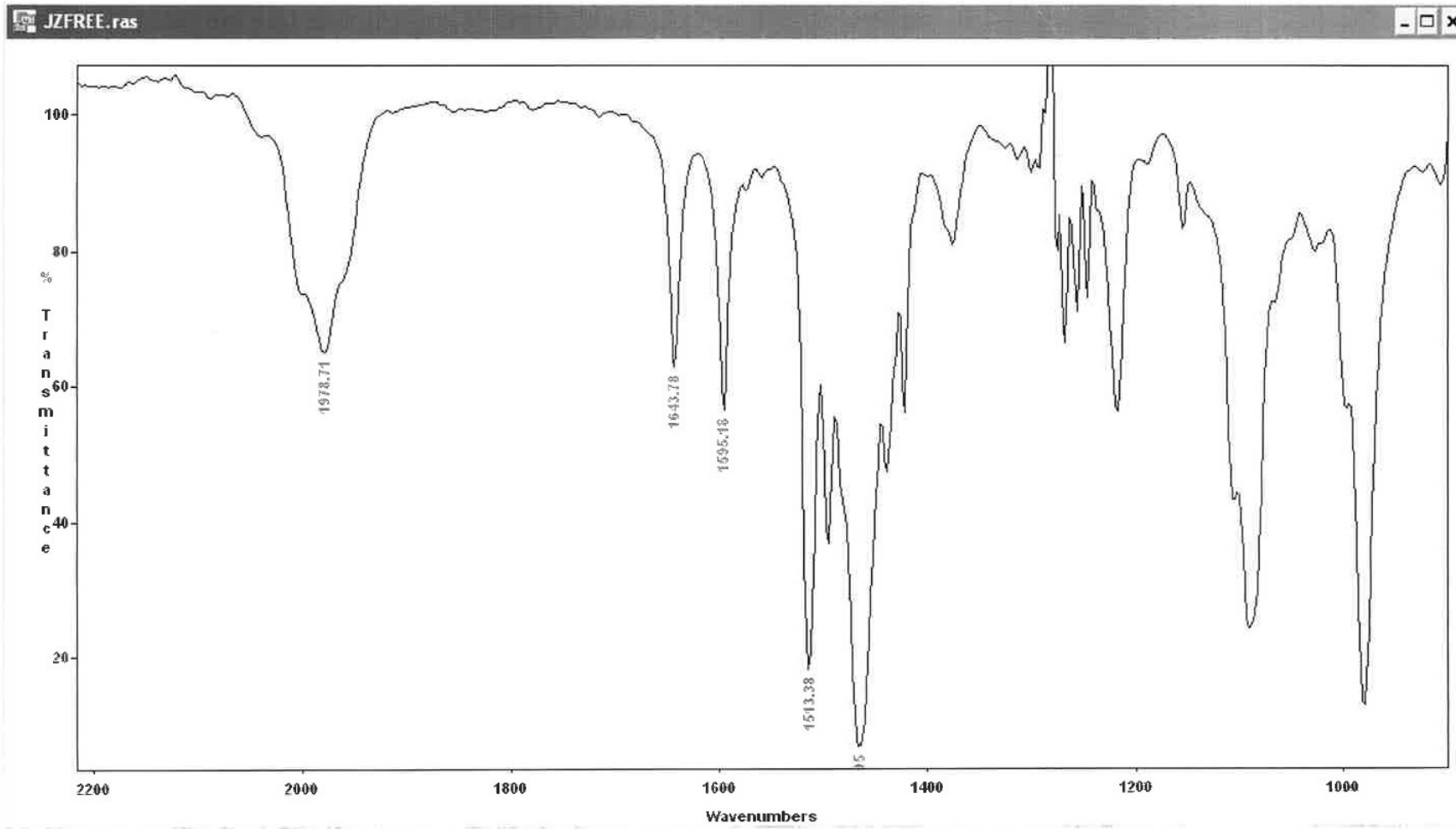


Figure S29. Infrared spectrum of [(^PhP₂Si=)Ru(H)(CO)(PPh₃)][BArF] in CH₂Cl₂

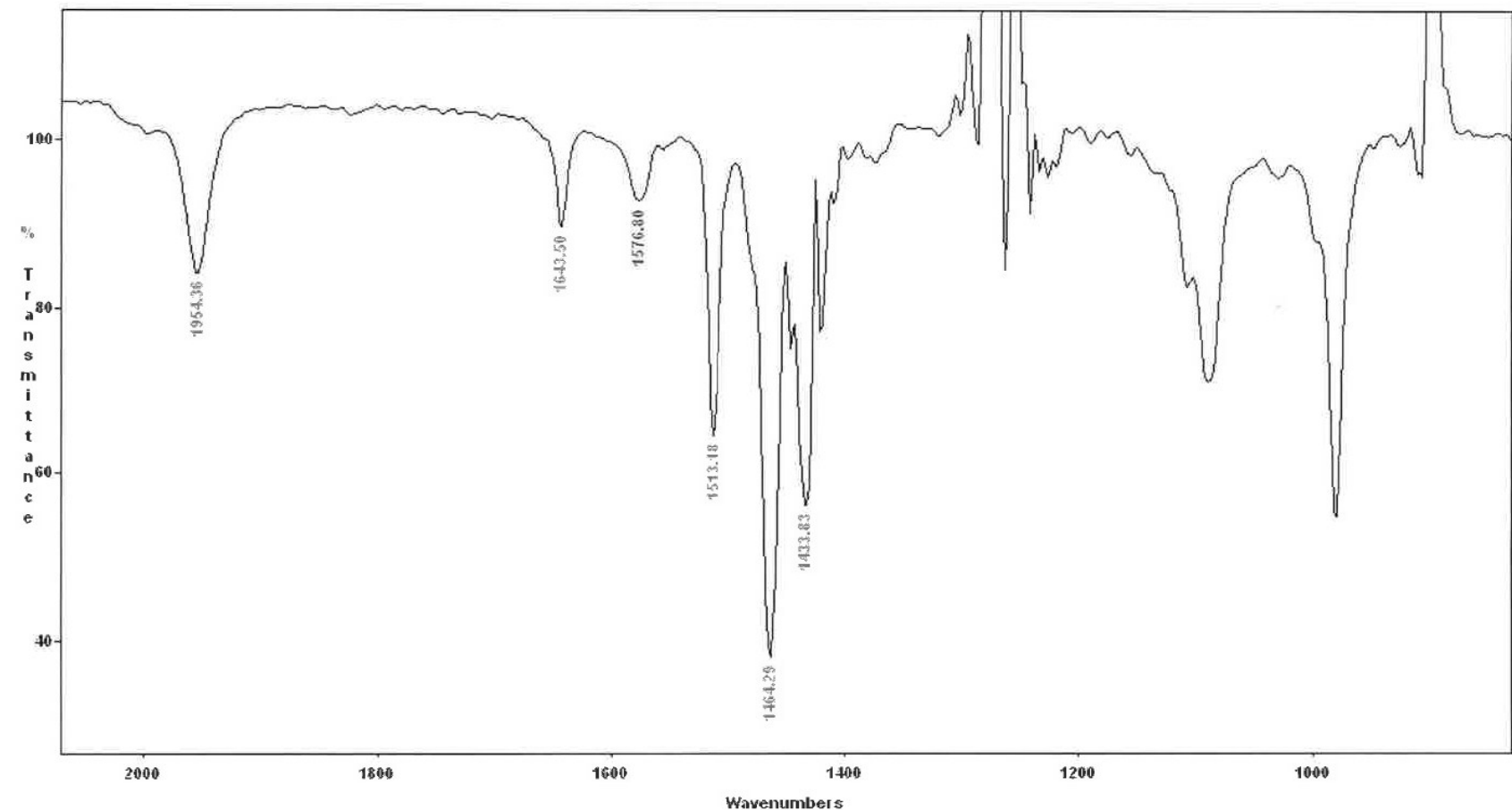


Figure S30. Infrared spectrum of $[(\text{Ph}_2\text{SiO}_2\text{CH})\text{Ru}(\text{H})(\text{CO})(\text{PPh}_3)][\text{BArF}]$ in CH_2Cl_2

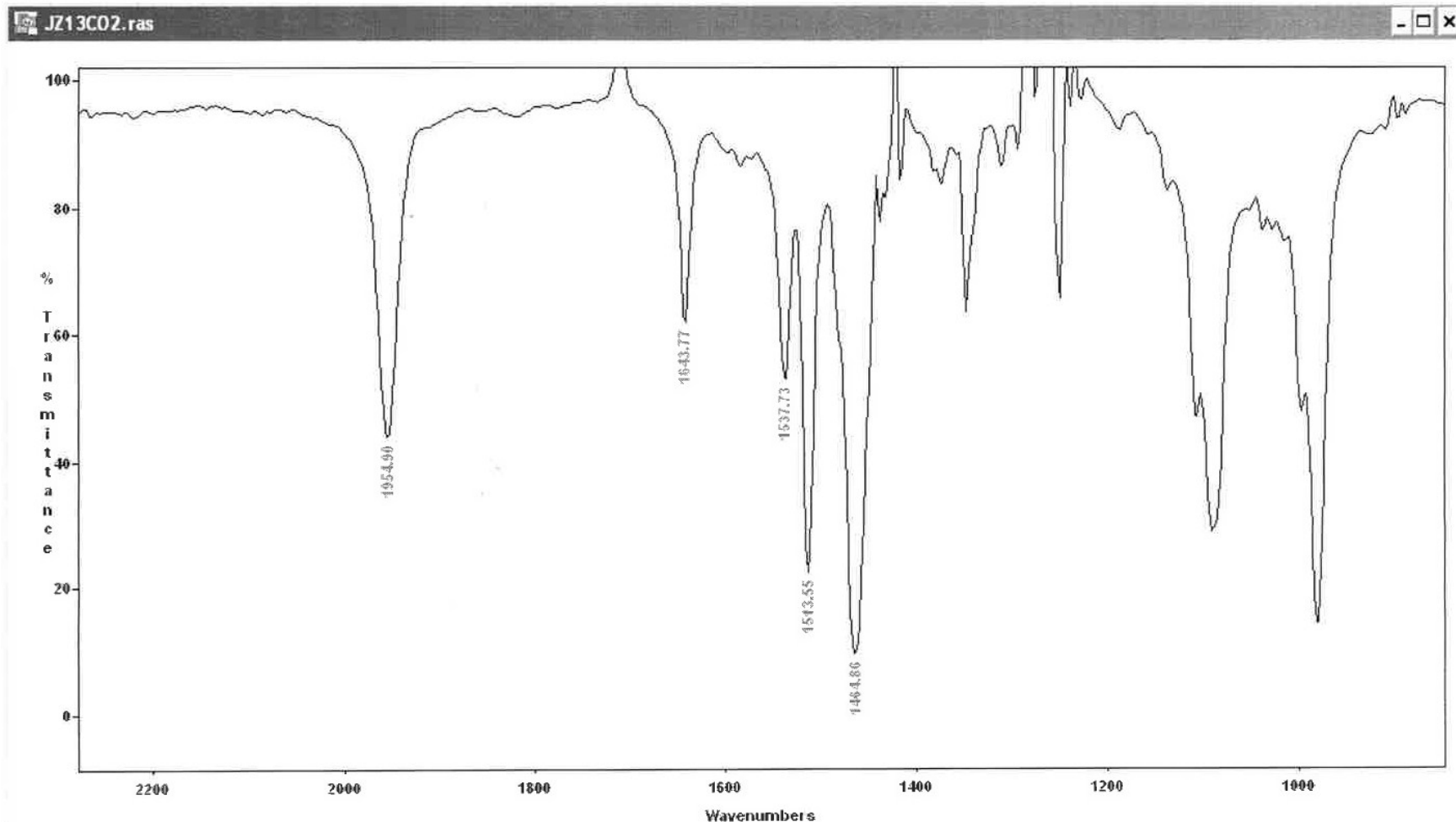


Figure S31. Infrared spectrum of ^{13}C -[$(^{\text{Ph}}\text{P}_2\text{Si}^{\text{O}2\text{CH}})\text{Ru}(\text{H})(\text{CO})(\text{PPh}_3)$][BArF] in CH_2Cl_2

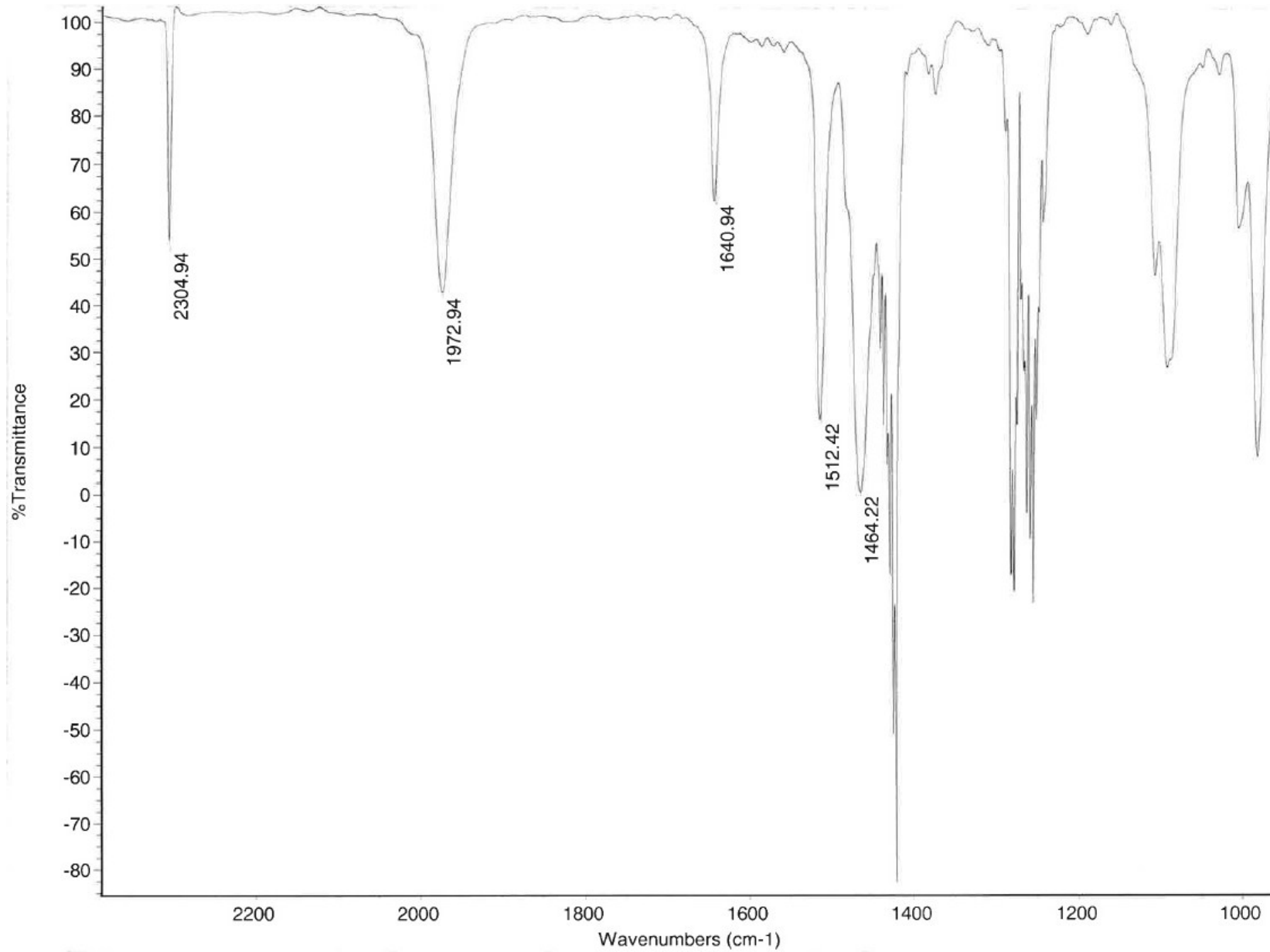


Figure S32. Infrared spectrum of $[(\text{PhP}_2\text{Si}^{\text{S}2\text{CH}})\text{Ru}(\text{H})(\text{CO})(\text{PPh}_3)][\text{BArF}]$ in CH_2Cl_2

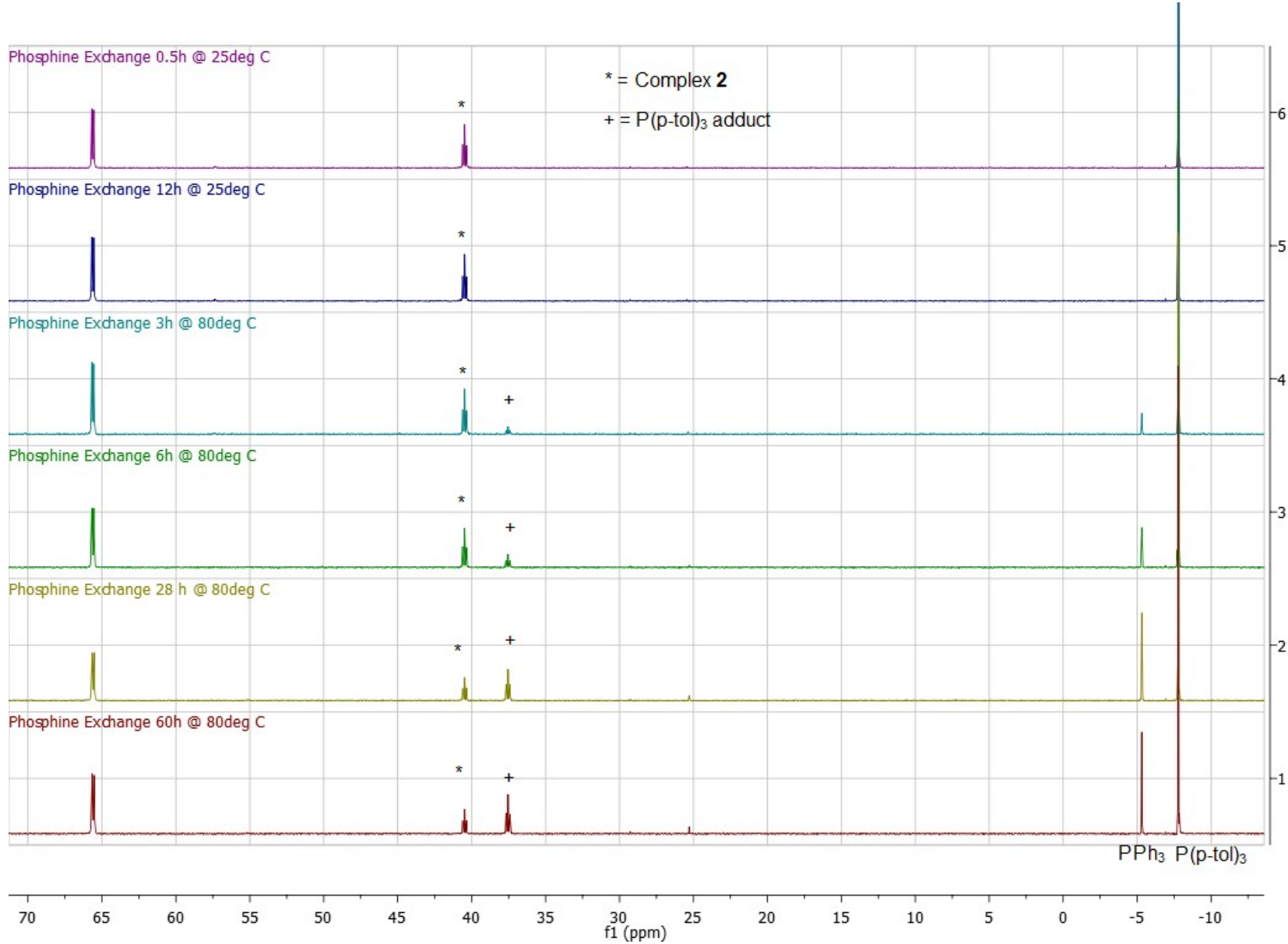


Figure S33. ³¹P NMR spectra of reaction of **2** with tri(*p*-tolyl)phosphine in C₆H₅F

References

- (1) Gu, W. X.; Ozerov, O. V. *Inorg. Chem.* **2011**, *50*, 2726.
- (2) Whited, M. T.; Deetz, A. M.; Boerma, J. W.; DeRosha, D. E.; Janzen, D. E. *Organometallics* **2014**, *33*, 5070.
- (3) Straus, D. A.; Zhang, C.; Tilley, T. D. *J. Organomet. Chem.* **1989**, *369*, C13.
- (4) Chien, J. C. W.; Tsai, W. M.; Rausch, M. D. *J. Am. Chem. Soc.* **1991**, *113*, 8570.
- (5) Frisch, M. J.; Trucks, G. W.; Schlegel, H. B.; Scuseria, G. E.; Robb, M. A.; Cheeseman, J. R.; Scalmani, G.; Barone, V.; Mennucci, B.; Petersson, G. A.; Nakatsuji, H.; Caricato, M.; Li, X.; Hratchian, H. P.; Izmaylov, A. F.; Bloino, J.; Zheng, G.; Sonnenberg, J. L.; Hada, M.; Ehara, M.; Toyota, K.; Fukuda, R.; Hasegawa, J.; Ishida, M.; Nakajima, T.; Honda, Y.; Kitao, O.; Nakai, H.; Vreven, T.; Montgomery Jr., J. A.; Peralta, J. E.; Ogliaro, F.; Bearpark, M. J.; Heyd, J.; Brothers, E. N.; Kudin, K. N.; Staroverov, V. N.; Kobayashi, R.; Normand, J.; Raghavachari, K.; Rendell, A. P.; Burant, J. C.; Iyengar, S. S.; Tomasi, J.; Cossi, M.; Rega, N.; Millam, N. J.; Klene, M.; Knox, J. E.; Cross, J. B.; Bakken, V.; Adamo, C.; Jaramillo, J.; Gomperts, R.; Stratmann, R. E.; Yazyev, O.; Austin, A. J.; Cammi, R.; Pomelli, C.; Ochterski, J. W.; Martin, R. L.; Morokuma, K.; Zakrzewski, V. G.; Voth, G. A.; Salvador, P.; Dannenberg, J. J.; Dapprich, S.; Daniels, A. D.; Farkas, Ö.; Foresman, J. B.; Ortiz, J. V.; Cioslowski, J.; Fox, D. J. *Gaussian 09*, Gaussian, Inc.: Wallingford, CT, USA, 2009.
- (6) Zhao, Y.; Truhlar, D. G. *Theor. Chem. Acc.* **2008**, *120*, 215.
- (7) (a) Weigend, F. *Physical Chemistry Chemical Physics* **2006**, *8*, 1057. (b) Weigend, F.; Ahlrichs, R. *Physical Chemistry Chemical Physics* **2005**, *7*, 3297.
- (8) Andrae, D.; Haussermann, U.; Dolg, M.; Stoll, H.; Preuss, H. *Theor. Chim. Acta* **1990**, *77*, 123.
- (9) *CrystalClear*, Rigaku Americas and Rigaku: The Woodlands, TX, 2011.
- (10) Dolomanov, O. V.; Bourhis, L. J.; Gildea, R. J.; Howard, J. A. K.; Puschmann, H. *J. Appl. Cryst.* **2009**, *42*, 339.
- (11) Farrugia, L. J. *J. Appl. Cryst.* **2012**, *45*, 849.
- (12) *Persistence of Vision Raytracer (Version 3.6)*, Persistence of Vision Pty. Ltd.: 2004.